

## Electronic Supplementary Information

for

# A family of twelve-membered ring photoswitches with excellent $Z \rightarrow E$ conversion

Ruben Falkenburg,<sup>‡a</sup> Maximilian J. Notheis,<sup>‡a</sup> Gregor Schnakenburg<sup>b</sup> and Larissa K. S. von Krbek<sup>\*a</sup>

- a. Kekulé-Institut für Organische Chemie and Biochemie, Rheinische Friedrich-Wilhelms-Universität Bonn, Gerhard-Domagk-Str. 1, 53121 Bonn, Germany.

E-mail: [larissa.vonkrbek@uni-bonn.de](mailto:larissa.vonkrbek@uni-bonn.de).

- b. Institut für Anorganische Chemie, Rheinische Friedrich-Wilhelms-Universität Bonn, Gerhard-Domagk-Str. 1, 53121 Bonn

‡ These authors contributed equally.

## Contents

1.	General procedures .....	3
2.	Synthetic procedures.....	5
2.1.	2,2'-(1,2-phenylenebis(ethyne-2,1-diyl))dianiline (S1).....	5
2.2.	2,2'-(1,2-phenylenebis(ethane-2,1-diyl))dianiline (C) .....	7
2.3.	2,2'-(1,2-phenylenebis(ethane-2,1-diyl))bis(4-iodoaniline) (D).....	9
2.4.	( <i>E</i> )-11,12,17,18-tetrahydrotribenzo[ <i>c,g,k</i> ][1,2]diazacyclododecine (1) .....	11
2.5.	Unsuccessful attempts to synthesize 1 .....	13
2.6.	General procedure for the ortho alkoxylation of cyclic azobenzene 1 .....	15
2.7.	( <i>E</i> )-4,7-dimethoxy-11,12,17,18-tetrahydrotribenzo[ <i>c,g,k</i> ][1,2]diazacyclo-dodecine (2) .....	16
2.8.	( <i>E</i> )-4,7-bis(2,2,2-trifluoroethoxy)-11,12,17,18-tetrahydrotribenzo[ <i>c,g,k</i> ][1,2]-diazacyclododecine (3) .....	18
2.9.	( <i>E</i> )-11,12,17,18-tetrahydrotribenzo[ <i>c,g,k</i> ][1,2]diazacyclododecine-4,7-diyl diacetate (4).....	21
2.10.	( <i>E</i> )-2,9-diiodo-11,12,17,18-tetrahydrotribenzo[ <i>c,g,k</i> ][1,2]diazacyclododecine (5) .....	23
2.11.	( <i>E</i> )-2,9-bis(ethylthio)-11,12,17,18-tetrahydrotribenzo[ <i>c,g,k</i> ][1,2]diazacyclo-dodecine (6) .....	25
2.12.	( <i>E</i> )-4,4'-(11,12,17,18-tetrahydrotribenzo[ <i>c,g,k</i> ][1,2]diazacyclododecine-2,9-diyl)bis( <i>N,N</i> -bis(4-methoxyphenyl)aniline) (7).....	27
3.	Photophysical characterization .....	30
3.1.	General procedures for the illumination of different types of samples.....	30
3.2.	NMR measurements of irradiated samples .....	31
3.2.1.	Cyclic azobenzene 1 .....	32
3.2.2.	Diiodo cyclic azobenzene 5.....	34
3.3.	Determination of photostationary states (PSS) by HPLC and UV-vis spectroscopy .....	36
3.3.1.	Cyclic azobenzene 1 .....	38
3.3.2.	Dimethoxy cyclic azobenzene 2 .....	40
3.3.3.	Bis(trifluoroethoxy) cyclic azobenzene 3 .....	41
3.3.4.	Diaceto cyclic azobenzene 4.....	43
3.3.5.	Diiodo cyclic azobenzene 5.....	45
3.3.6.	Thioether substituted cyclic azobenzene 6.....	47
3.3.7.	bis(4-methoxyphenyl)phenylamine substituted cyclic azobenzene 7 .....	49
3.4.	Determination of thermal half-lives $\tau_{1/2}$ by UV-Vis and $^1\text{H}$ NMR spectroscopy .....	50
3.5.	Reversibility of photoisomerization.....	54
4.	Quantum chemical calculations .....	55
5.	Crystal structure .....	56
6.	References.....	58

## 1. General procedures

**Reagents and materials.** Commercial solvents and reagents were obtained from the following suppliers and used without further purification unless specified otherwise: Sigma Aldrich, Alfa Aesar, abcr, Acros Organics, BLD-Pharm, Fluorochem, Merck, TCI, Carbolution, Thermo Fisher Scientific.

Dry solvents (acetonitrile, tetrahydrofuran, methanol) were dried using a MP-SPS 800 (MBraun) drying apparatus. Solvents used for column chromatography were distilled at atmospheric pressure prior to use.

**Schlenk techniques.** All reactions using chemicals sensitive to air were carried out under argon using established Schlenk techniques. If chemicals were also sensitive to moisture, glassware was flame-dried prior to use.

**Column chromatography.** Column chromatography was carried out either using a puriFlash 5.020 (Interchim) flash chromatography machine with PuriFlash 15  $\mu\text{m}$  Si HP (Interchim) flash cartridges or by hand using Silica gel ultra pure (Thermo scientific, 60  $\mu\text{m}$ ).

**HPLC.** Analytical HPLC runs were carried out on a Prominence Modular HPLC (Shimadzu) using a YMC-Pack Pro C18 (spherical, 3  $\mu\text{m}$ ) column with 0.5 mL  $\text{min}^{-1}$  flow rate of  $\text{CH}_3\text{OH} / \text{CH}_3\text{CN}$  (1:1 (v:v)) using the built-in UV-vis detector.

**NMR spectroscopy.** All NMR spectroscopic measurements were carried out using 300 MHz, 400 MHz, 500 MHz or 700 MHz spectrometers (Bruker Avance I 300, Bruker Avance I 400, Bruker Avance I 500, Bruker Avance III HD Prodigy 500, Bruker Avance III HD Ascend 700).  $^1\text{H}$  and  $^{13}\text{C}$  NMR spectra are referenced to the residual solvent peak for  $\text{CD}_3\text{CN}$  ( $^1\text{H}$ : 1.94 ppm,  $^{13}\text{C}$ : 1.32 ppm),  $\text{CD}_2\text{Cl}_2$  ( $^1\text{H}$ : 5.32 ppm,  $^{13}\text{C}$ : 53.5 ppm) or  $\text{CDCl}_3$  ( $^1\text{H}$ : 7.26 ppm,  $^{13}\text{C}$ : 77.16 ppm). NMR signals are reported in terms of chemical shift ( $\delta$ ) in ppm, relative integral, multiplicity, coupling constants (in Hz) and assignment, in that order. The following abbreviations for multiplicity are used: s, singlet; d, doublet; t, triplet; qu, quartet; qn, quintet; m, multiplet; br, broad. Spectra were digitally processed (phase and baseline corrections, integration, peak analysis) using MestReNova 14.2.1 (Mestrelab) and TopSpin 4.05 (BrukerBioSpin) were used to evaluate and plot the data. All processing operations were manually checked to ensure that the processed spectra accurately represented the raw data.

**Mass spectrometry.** Mass spectra were acquired using an Orbitrap XL (Thermo Fischer Scientific) and evaluated and plotted using XCalibur 4.2 (Thermo Fischer Scientific).

**UV-vis spectroscopy.** UV-vis spectroscopy was carried out using a Clariostar Plus (BMG Labtech) plate reader utilizing a flash lamp style spectrometer.

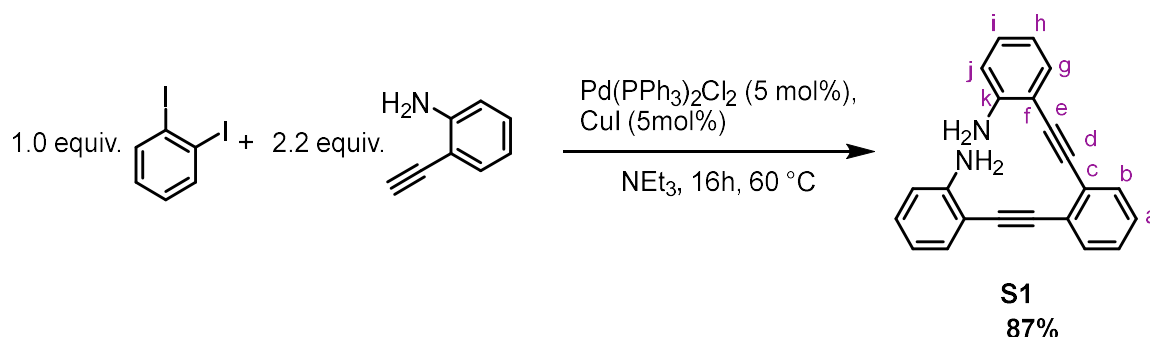
**Light sources.** Illumination experiments were carried out using Prizmatrix fiber collimated LEDs.

Table S1. Light output of used LEDs.

$\lambda$ [nm]	310	325	365	390	405	430	450	500	590	660	white
Output power (1 m optical fiber) [mW]	8.6	13	170	220	260	160	440	165	230	140	74

## 2. Synthetic procedures

### 2.1. 2,2'-(1,2-phenylenebis(ethyne-2,1-diyl))dianiline (S1)



2,2'-(1,2-phenylenebis(ethyne-2,1-diyl))dianiline (**S1**) was synthesized after a modified literature procedure for analogous reactions.<sup>1</sup>

Triethylamine (15 mL) was deoxygenated by bubbling under a stream of Ar for 15 min. Bis(triphenylphosphine)palladium(II) dichloride (0.05 equiv., 27.8 mg, 39.7  $\mu\text{mol}$ ), copper iodide (0.05 equiv., 7.9 mg, 41.5  $\mu\text{mol}$ ), 1,2-diiodobenzene (1.00 equiv., 247 mg, 750  $\mu\text{mol}$ ), and 2-ethynylaniline (2.20 equiv., 220 mg, 1.88 mmol) were added to the triethylamine and the mixture deoxygenated a second time by bubbling under a stream of Argon for 20 min. The yellow reaction mixture was stirred at 60  $^\circ\text{C}$  for 16 h. Subsequently, the solution was allowed to cool to room temperature before purification. All volatiles were removed from the reaction mixture under reduced pressure on a rotary evaporator, the crude product was dissolved in dichloromethane, and filtered over a short silica plug (5 cm diameter, 5 cm height) with DCM to afford diamine **S1** as a brown oil (200 mg, 648  $\mu\text{mol}$ , 87%).

$\text{C}_{22}\text{H}_{16}\text{N}_2$  308.38  $\text{g mol}^{-1}$

$R_F$  value (cyclohexane:ethyl acetate; (8:2 (v/v)) = 0.30.

$^1\text{H NMR}$  (500 MHz,  $\text{CD}_2\text{Cl}_2$ , 298 K):  $\delta_{\text{H}}$  [ppm] = 4.40 (s, 4H,  $\text{NH}_2$ ), 6.74 – 6.67 (m, 4H, H-j,h), 7.19 – 7.13 (m, 2H, H-i), 7.39 – 7.31 (m, 4H, H-b,g), 7.57 – 7.64 (m, 2H, H-a).

$^{13}\text{C NMR}$  (126 MHz,  $\text{CD}_2\text{Cl}_2$ , 298 K):  $\delta_{\text{C}}$  [ppm] = 90.47, 94.09, 107.39, 114.52, 117.93, 128.50, 130.54, 132.15, 132.43, 148.88.

$\text{HRMS}$  (ESI<sup>+</sup>-Orbitrap):  $m/z$  (relative intensity) = 309.1377 (100%,  $[\text{M}+\text{H}]^+$ , calcd 309.1386).

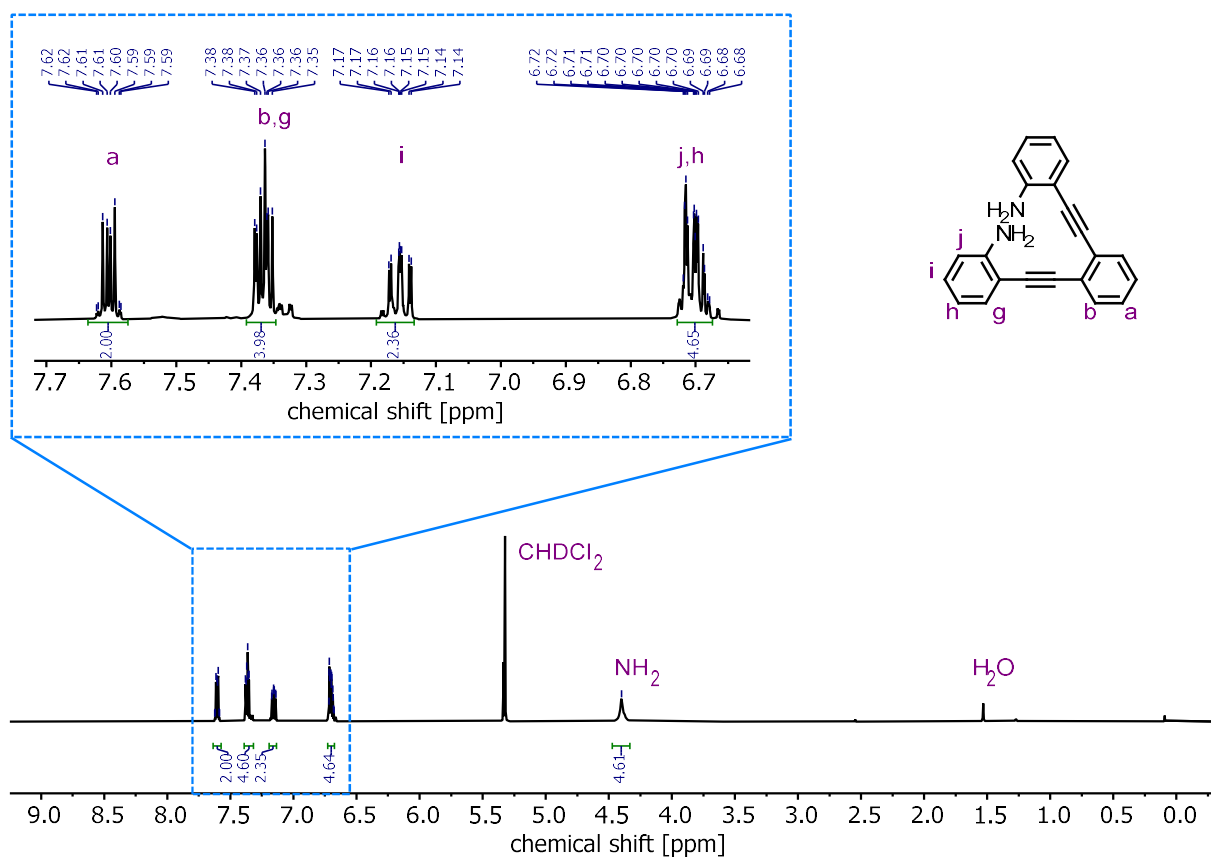


**Figure S1.** <sup>1</sup>H NMR spectrum (500 MHz, CD<sub>2</sub>Cl<sub>2</sub>, 298 K) of dianiline **S1**.

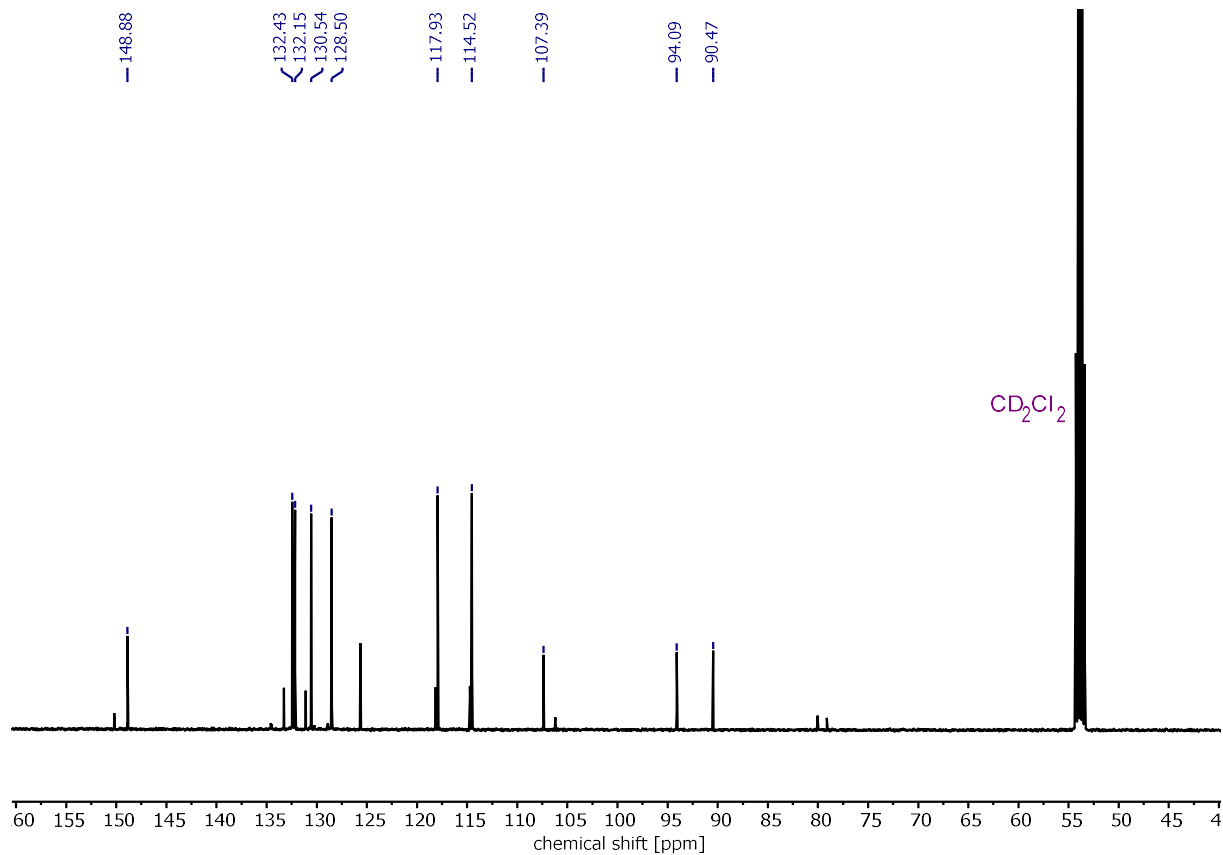
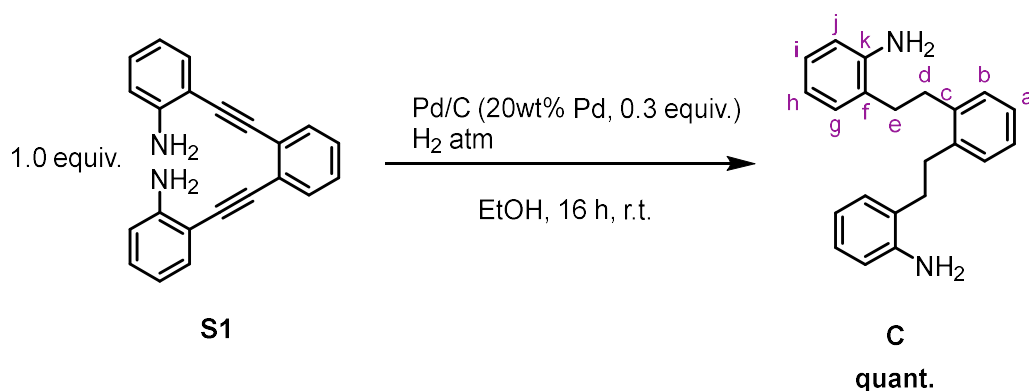


**Figure S2.** <sup>13</sup>C NMR spectrum (126 MHz, CD<sub>2</sub>Cl<sub>2</sub>, 298 K) of dianiline **S1**.

## 2.2. 2,2'-(1,2-phenylenebis(ethane-2,1-diyl))dianiline (C)



2,2'-(1,2-phenylenebis(ethane-2,1-diyl))dianiline (**C**) was synthesized after a modified literature procedure for analogous reactions.<sup>1</sup>

Diamine **ESI-1** (200 mg, 648  $\mu$ mol, 1.0 equiv.) and Pd/C (20%<sup>w</sup>t Pd, 100 mg, 189  $\mu$ mol, 0.3 equiv.) were suspended in 25 mL ethanol. The reaction mixture was purged with hydrogen and stirred for 16 h under a hydrogen atmosphere. The volatiles were removed from the reaction mixture under reduced pressure at a rotary evaporator. The obtained crude product was dissolved in EtOAc (5 mL) filtered over a silica plug (5 cm diameter, 5 cm height) using EtOAc (150 mL). Removing the solvent from the obtained filtrate under reduced pressure on a rotary evaporator afforded diamine **C** as a brown oil (202 mg, 648  $\mu$ mol, quant.).

**C**<sub>22</sub>**H**<sub>24</sub>**N**<sub>2</sub>                      316.45 g mol<sup>-1</sup>

**R<sub>F</sub> value** (cyclohexane:ethyl acetate; 8:2 (v/v)) = 0.18.

<sup>1</sup>**H NMR** (500 MHz, CD<sub>2</sub>Cl<sub>2</sub>, 298 K):  $\delta_{\text{H}}$  [ppm] = 2.71 – 2.78 (m, 4H, H-e), 2.91 – 2.97 (m, 4H, H-d), 3.61 (s, 4H, NH<sub>2</sub>), 6.67 (dd, J = 8.3, 1.3 Hz, 2H, H-j), 6.71 (td, J = 7.4, 1.2 Hz, 2H, H-h), 6.99 – 7.06 (m, 4H, H-g,i), 7.16 – 7.21 (m, 2H, H-a), 7.21 – 7.25 (m, 2H, H-b).

<sup>13</sup>**C NMR** (126 MHz, CD<sub>2</sub>Cl<sub>2</sub>, 298 K):  $\delta_{\text{C}}$  [ppm] = 27.33, 32.19, 33.41, 115.90, 118.99, 126.49, 126.69, 127.47, 129.67, 129.78, 140.24, 144.91.

**HRMS** (ESI<sup>+</sup>-Orbitrap):  $m/z$  (relative intensity) = 317.2012 (100%, [M+H]<sup>+</sup>, calcd 317.2012).

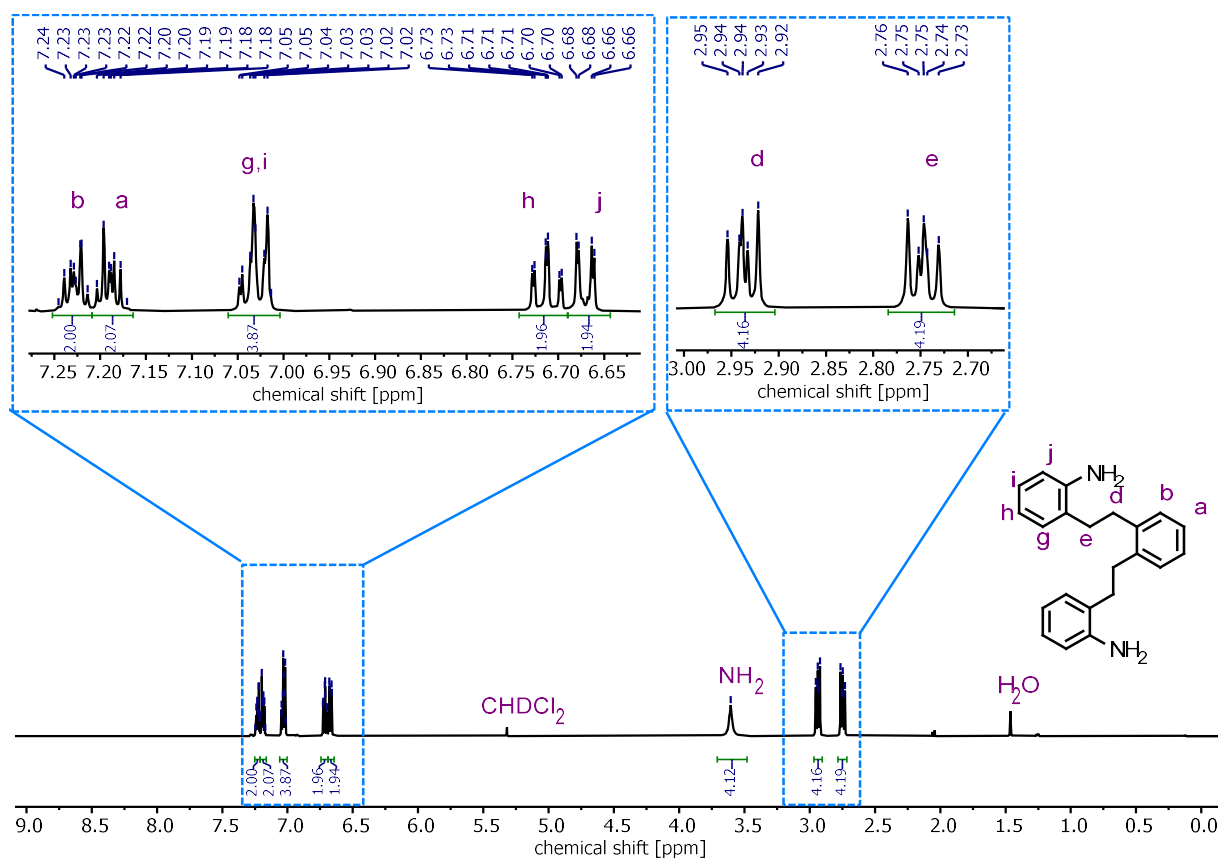


**Figure S3.**  $^1\text{H}$  NMR spectrum (500 MHz,  $\text{CD}_2\text{Cl}_2$ , 298 K) of dianiline **C**.

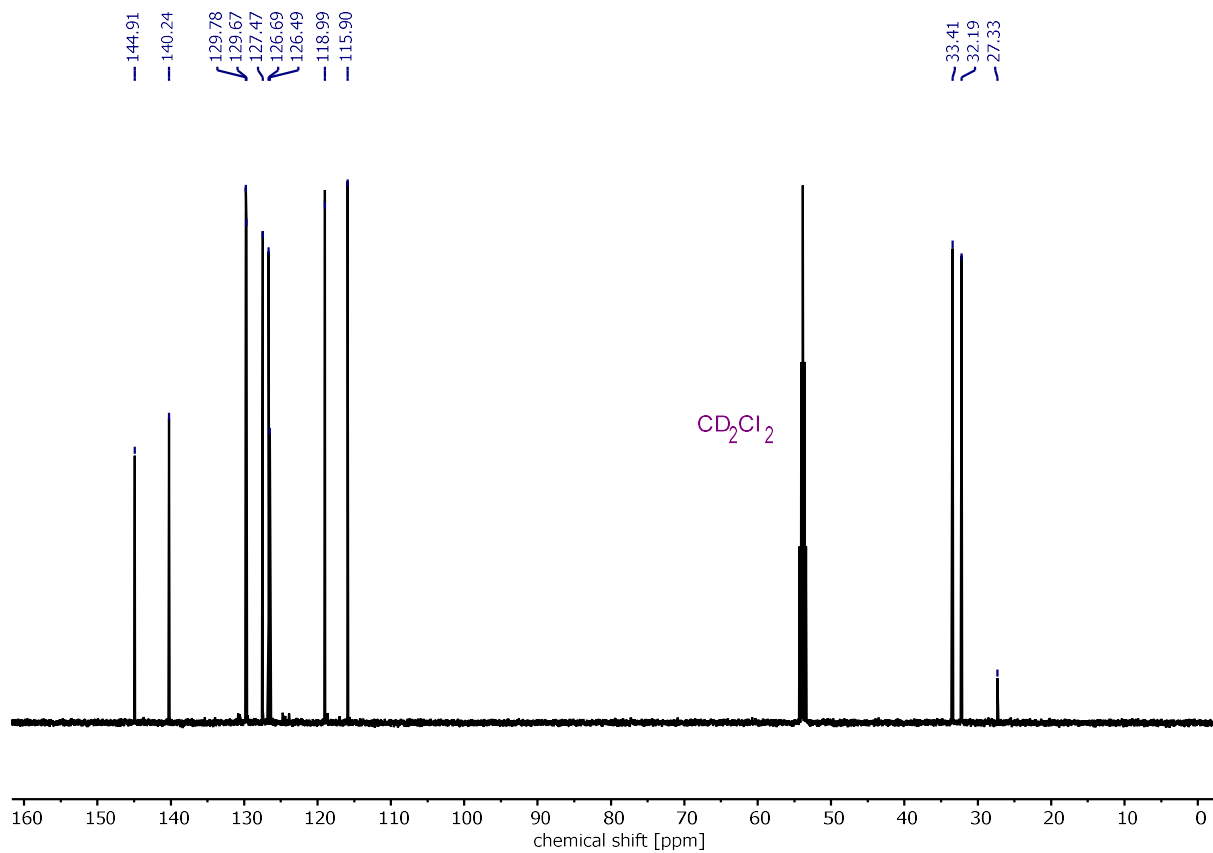
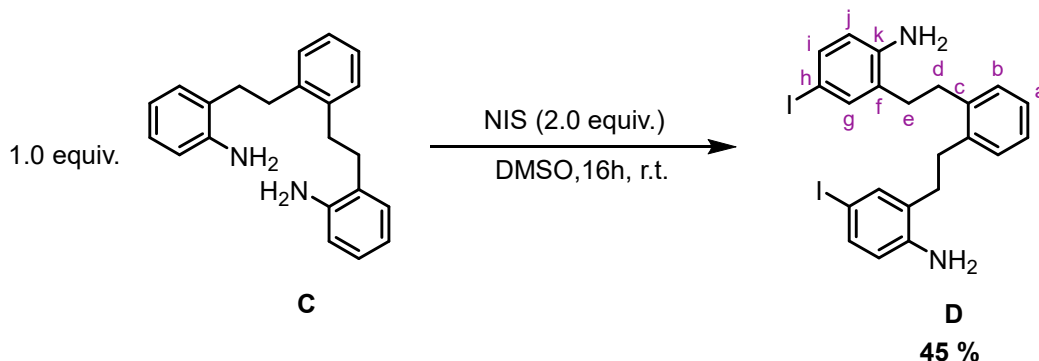


**Figure S4.**  $^{13}\text{C}$  NMR spectrum (126 MHz,  $\text{CD}_2\text{Cl}_2$ , 298 K) of dianiline **C**.



### 2.3. 2,2'-(1,2-phenylenebis(ethane-2,1-diyl))bis(4-iodoaniline) (D)



2,2'-(1,2-phenylenebis(ethane-2,1-diyl))bis(4-iodoaniline) (**D**) was synthesized after a modified literature procedure for analogous reactions.<sup>1</sup>

*N*-iodosuccinimide (524 mg, 2.33 mmol, 2.01 equiv.) was added to a solution of **C** (367 mg, 1.16 mmol, 1.0 equiv.) in DMSO (25 mL). After stirring for 16 h at room temperature, a water/saturated aqueous sodium chloride solution (4:1, 50 mL) was added to the reaction mixture and the resulting water/DMSO mixture extracted with dichloromethane (3×30 mL). The combined organic phases were dried over sodium sulfate. The solvent was removed under reduced pressure a rotary evaporator and the residue purified by column chromatography (0 to 30% ethyl acetate in cyclohexane) to afford the title compound **D** as a yellow oil (298 mg, 0.524 mmol, 45%).

$\text{C}_{22}\text{H}_{22}\text{I}_2\text{N}_2$                        $568.24 \text{ g mol}^{-1}$

**R<sub>F</sub> value** (cyclohexane:ethyl acetate; 8:2 (v/v)) = 0.15.

**<sup>1</sup>H NMR** (500 MHz,  $\text{CD}_2\text{Cl}_2$ , 298 K):  $\delta_{\text{H}}$  [ppm] = 2.60 – 2.70 (m, 4H, H-e), 2.80 – 2.90 (m, 4H, H-d), 3.64 (s, 4H,  $\text{NH}_2$ ), 6.47 (dd,  $J = 7.9, 0.7 \text{ Hz}$ , 2H, H-j), 7.18 (s, 4H, H-a,b), 7.24 – 7.32 (m, 4H, H-g,i).

**<sup>13</sup>C NMR** (126 MHz,  $\text{CD}_2\text{Cl}_2$ , 298 K):  $\delta_{\text{C}}$  [ppm] = 31.87, 33.05, 79.86, 118.03, 126.92, 129.16, 129.71, 136.11, 138.17, 139.75, 144.75.

**HRMS** (ESI<sup>+</sup>-Orbitrap):  $m/z$  (relative intensity) = 568.9942 (100%,  $[\text{M}+\text{H}]^+$ , calcd 568.9945).

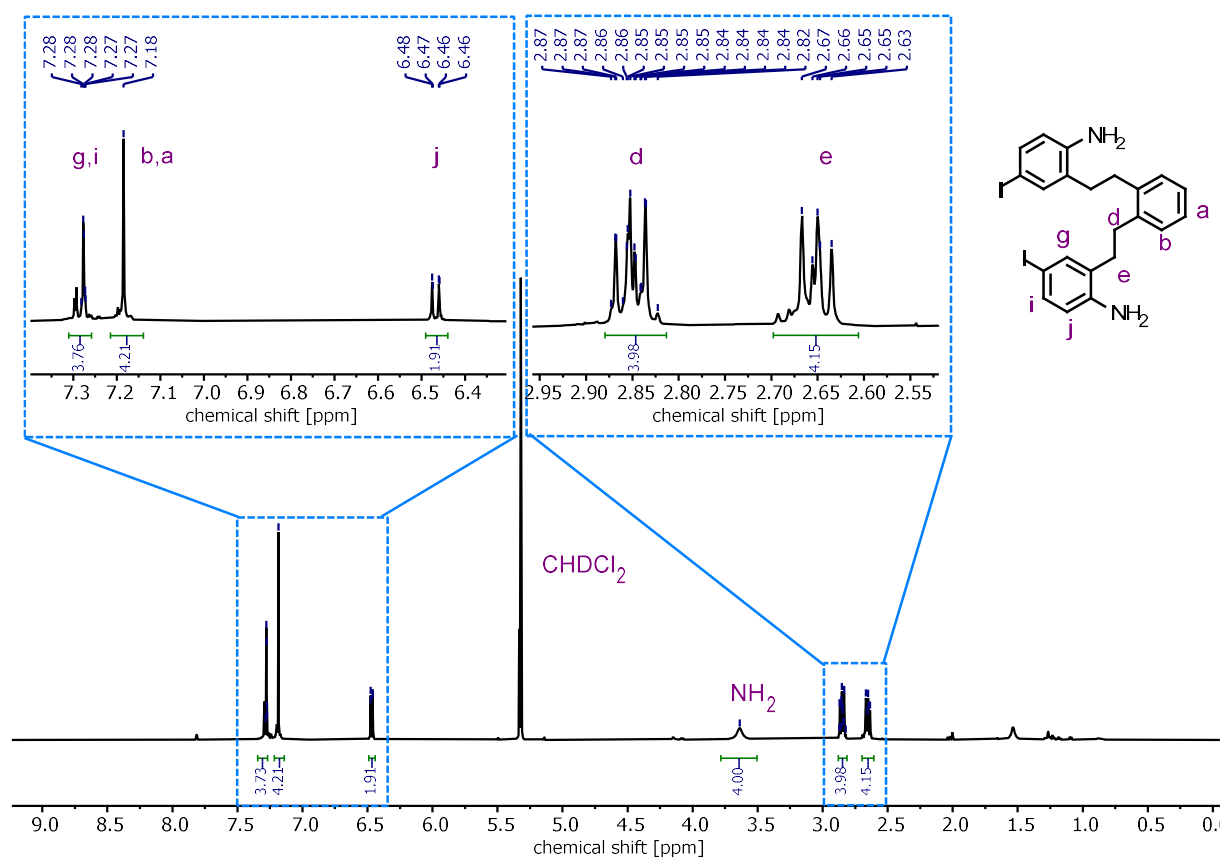


Figure S5.  $^1\text{H}$  NMR spectrum (500 MHz,  $\text{CD}_2\text{Cl}_2$ , 298 K) of diiodide D.

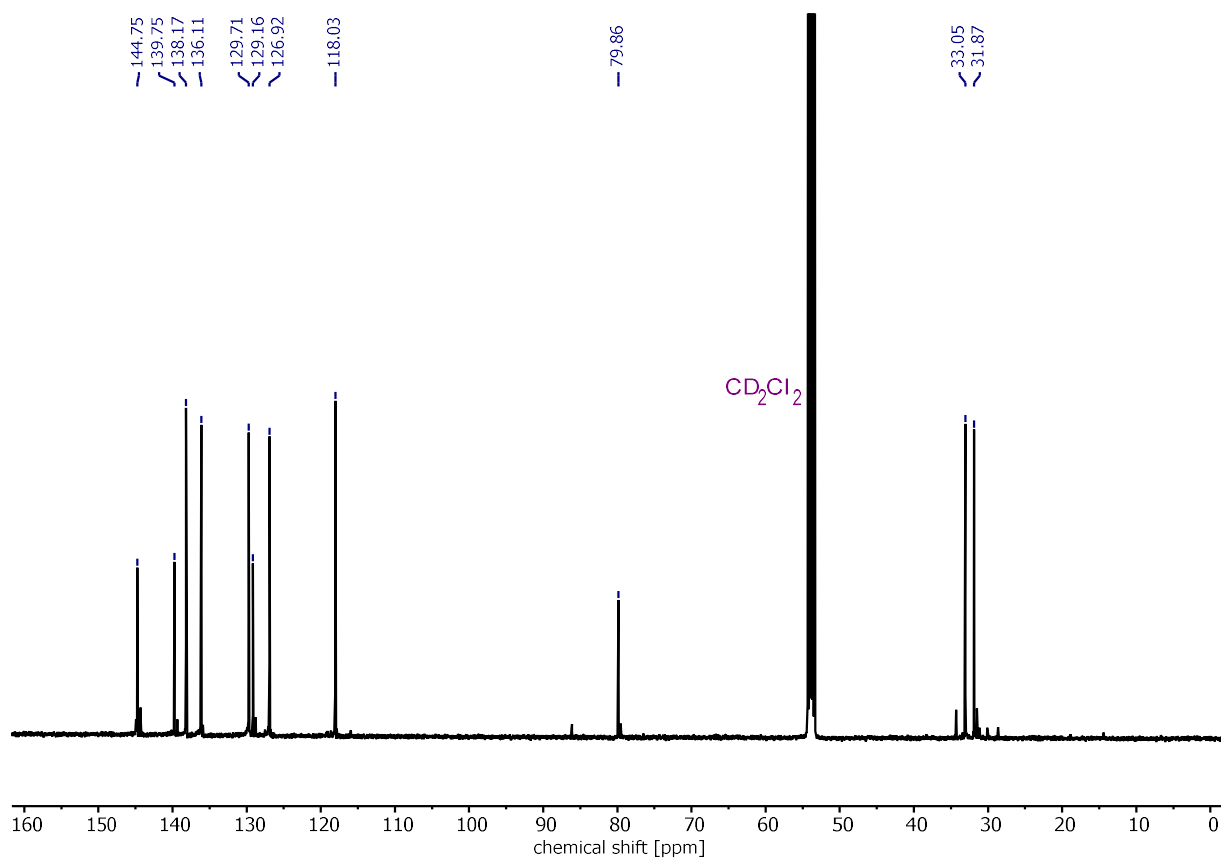
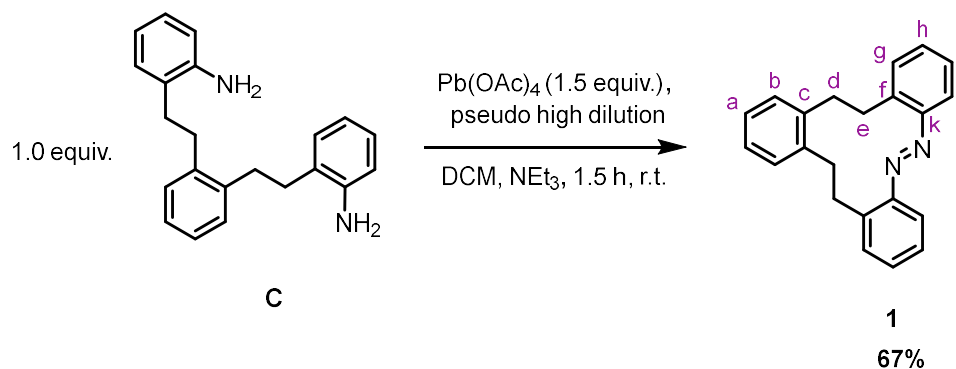


Figure S6.  $^{13}\text{C}$  NMR spectrum (126 MHz,  $\text{CD}_2\text{Cl}_2$ , 298 K) of diiodide D.

#### 2.4. (E)-11,12,17,18-tetrahydrotribenzo[c,g,k][1,2]diazacyclododecine (1)



A three-necked flask was equipped with two 250 mL dropping funnels. One funnel was loaded with a solution of dianiline **C** (134 mg, 0.423 mmol, 1.00 equiv., 3 mmol/L) and TEA (1 mL) in DCM (140 mL) and the other dropping funnel was loaded with a solution of lead(IV) acetate (296 mg, 0.634 mmol, 1.50 equiv., 6 mmol/L) in DCM (100 mL). Both solutions were added dropwise into DCM (250 mL) within 50 min\* at room temperature. After the addition was complete, the reaction mixture was stirred at room temperature for another 30 min. Afterwards the solvents were removed from the reaction mixture under reduced pressure on a rotary evaporator. The remaining residue was redissolved in cyclohexane and filtered over a silica plug (5 cm diameter, 5 cm height). The macrocyclic azobenzene **1** was obtained as an orange solid (89 mg, 0.285 mmol, 67%).



**R<sub>F</sub> value** (cyclohexane:ethyl acetate; 8:2 (v/v)) = 0.67.

**<sup>1</sup>H NMR** (500 MHz, CD<sub>2</sub>Cl<sub>2</sub>, 298 K) δ<sub>H</sub> [ppm] = 2.75 – 3.69 (m, 8H, H-e,d), 7.16 – 7.21 (m, 2H, H-a), 7.28 – 7.33 (m, 2H, H-b), 7.40 – 7.50 (m, 6H, H-g,h,i), 7.92 – 7.96 (m, 2H, H-j).

**<sup>13</sup>C NMR** (126 MHz, CD<sub>2</sub>Cl<sub>2</sub>, 298 K) δ<sub>C</sub> [ppm] = 36.69 (C-d), 38.02 (C-e), 124.30 (C-j), 126.67 (C-a), 127.55 (C-g/h/i), 130.50 (C-f), 130.97 (C-b), 131.81 (C-g/h/i), 137.84 (C-g/h/i), 140.78 (C-c), 151.31 (C-l). Due to their overlap in the <sup>1</sup>H NMR spectrum C-g, C-h and C-i could not be distinguished.

**HRMS** (ESI<sup>+</sup>-Orbitrap): m/z (relative intensity) = 313.1697 (100%, [M+H]<sup>+</sup>, calcd 313.1699).

\*The reaction is relatively robust. However, addition times between 10 and 50 minutes afforded the highest yields.

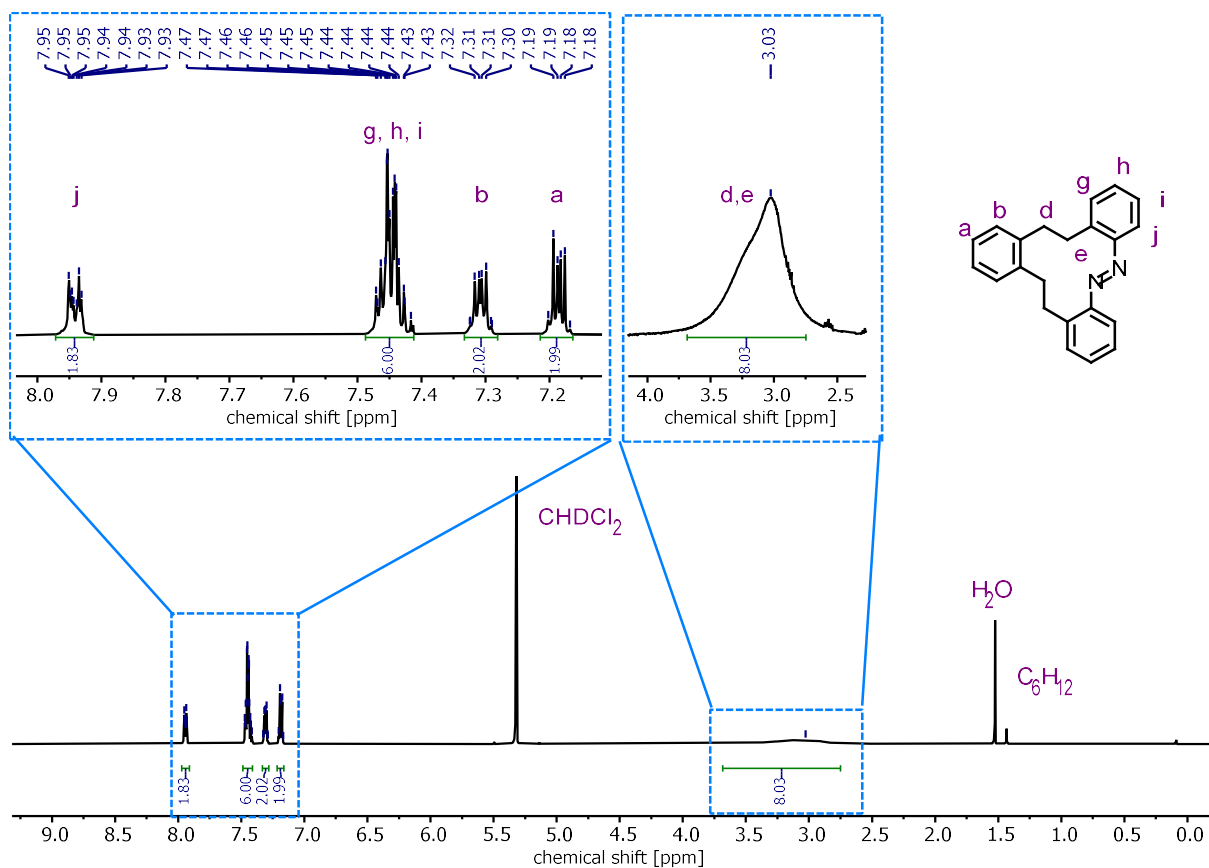


Figure S7.  $^1\text{H}$  NMR spectrum (500 MHz,  $\text{CD}_2\text{Cl}_2$ , 298 K) of cyclic azobenzene **1**.

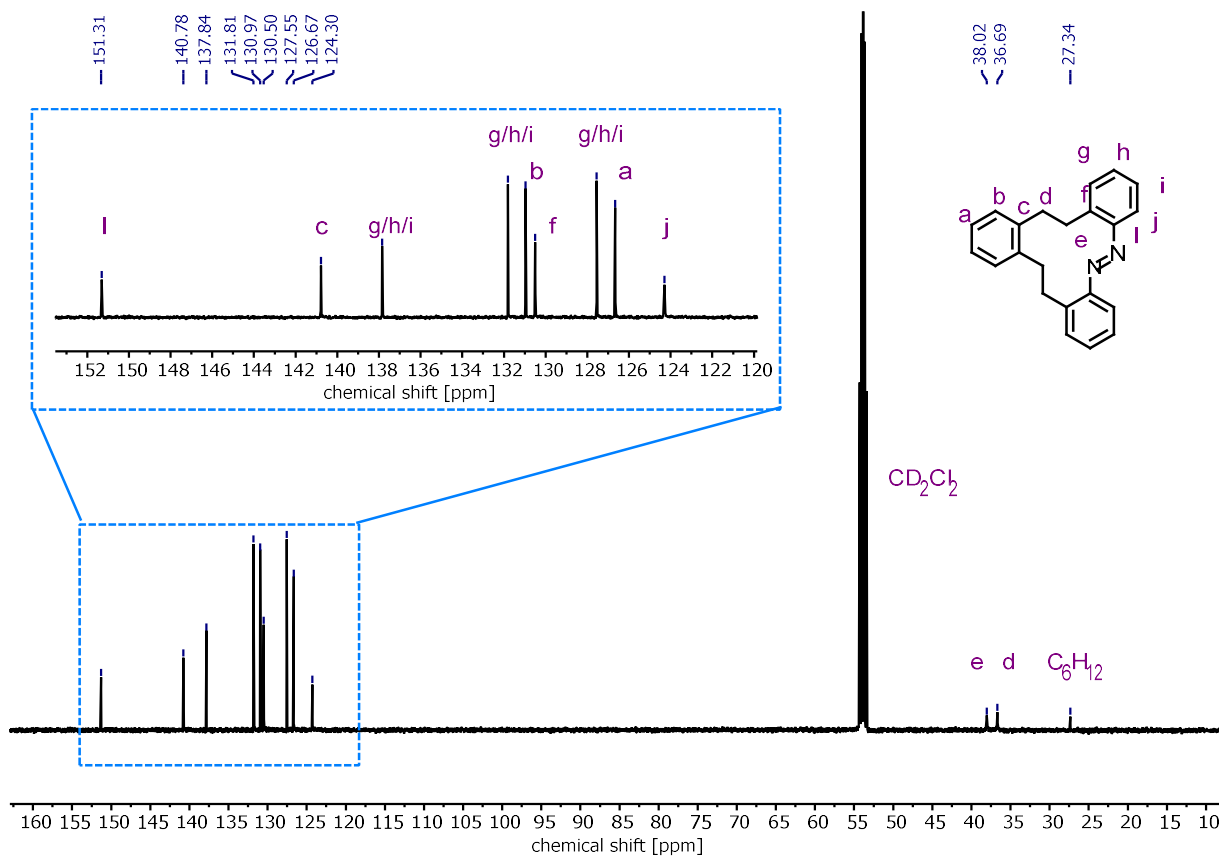
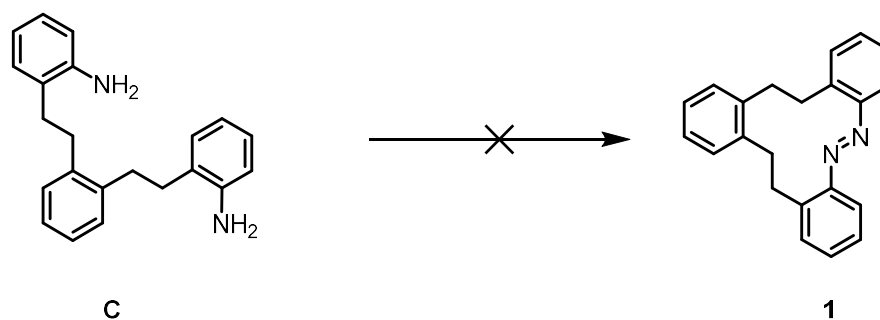


Figure S8.  $^{13}\text{C}$  NMR spectrum (126 MHz,  $\text{CD}_2\text{Cl}_2$ , 298 K) of cyclic azobenzene **1**.

## 2.5. Unsuccessful attempts to synthesize 1



### General procedure (a) for the oxidation of C

Dianiline **C** was dissolved in dry toluene (6 mL), the oxidant (2-6 equiv.) was added, and the suspension was heated to reflux for the indicated time. Then the reaction mixture was allowed to reach room temperature and was diluted with DCM (10 mL). The reaction mixture was filtered through celite. The filtrate was evaporated to dryness under reduced pressure, and the residue was chromatographed on silica gel with cyclohexane as eluent, to obtain the desired product.

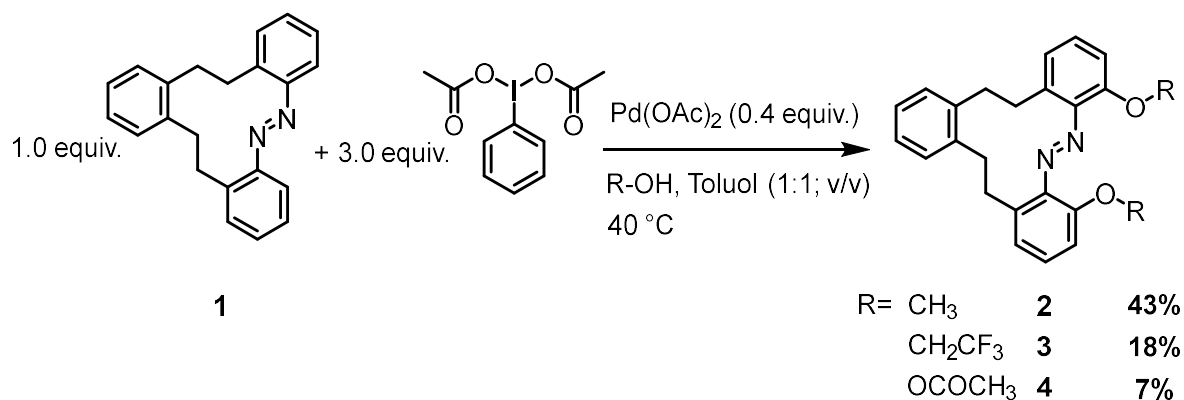
### General procedure (b) for the oxidation of C

A freshly prepared and titrated (0.57 – 0.62 M) solution of the oxidant (2.0 equiv.) in acetic acid was added to a solution of dianiline **C** in acetic acid/dichloromethane = 1/3 (6.25 mL) via a syringe pump within a period of **X** hours under rapid stirring. After the complete addition of the oxidant solution, the mixture was stirred for at least one more hour. The solvent was then removed under reduced pressure, the residue taken up in ethyl acetate (10 mL), and the ethyl acetate solution washed with saturated aqueous sodium hydrogen carbonate solution (2×5 mL), followed by saturated aqueous sodium chloride solution (5 mL). The organic layer was dried over sodium sulphate, the solvent was removed under reduced pressure, and the residue was purified by filtration over silica using cyclohexane as eluent.

**Table S2.** Overview over the reaction conditions tested for the synthesis of **5**.

<b>Oxidant</b>	<b>Reaction time</b>	<b>time for the addition of the oxidant</b>	<b>concentration of dianiline C</b> [mol L <sup>-1</sup> ]	<b>yield</b> [%]	<b>General procedure</b>
<b>Cu/O<sub>2</sub></b>	4 h	-	0.5	0	a
<b>Cu/O<sub>2</sub></b>	16 h	-	0.5	0	a
<b>Cu/air</b>	4 h		0.5	0	a
<b>Cu/air</b>	16 h		0.5	0	a
<b>tBuOCl</b>	1 h	5 min	0.26	0	b
<b>tBuOCl</b>	4 h	3h 30 min	0.26	0	b
<b>tBuOCl</b>	16 h	15 h 30 min	0.26	0	b
<b>MnO<sub>2</sub> dried at 80 °C</b>	8 h	-	0.52	0	a
<b>MnO<sub>2</sub> dried at 120 °C</b>	8 h	-	0.52	0	a
<b>MnO<sub>2</sub></b>	8 h	-	0.52	0	a
<b>mCPBA</b>	16 h	12 h	0.18-0.36	3	b
<b>mCPBA</b>	24 h	23 h	0.36	3	b
<b>mCPBA pseudo high dilution</b>	48 h	48 h	0.13	8	b
<b>mCPBA at 0 °C</b>	16 h	15 h 30min	0.36	5	b
<b>mCPBA at -78 °C</b>	16 h	12 h	0.36	0	b
<b>Pb(OAc)<sub>4</sub></b>	1.5 h	30 min	0.85	67	-

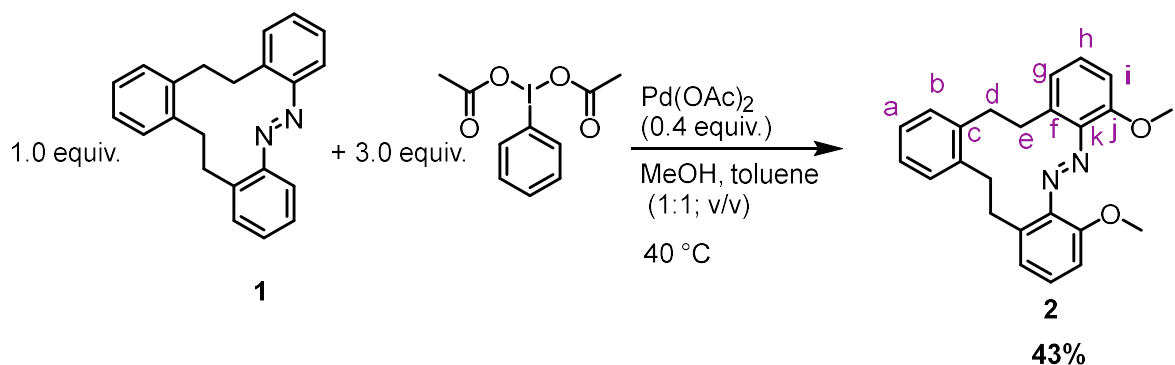
## 2.6. General procedure for the ortho alkoxylation of cyclic azobenzene 1



Derivatives **2**, **3**, and **4** were synthesized following a literature procedure<sup>2</sup> for the ortho alkoxylation of noncyclic azobenzenes.

Cyclic azobenzene **1** (1.0 equiv.), (diacetoxyiodo)benzene(phenyl)iodine(III) diacetate (PIDA; 3.0 equiv.) and palladium(II) acetate (0.4 equiv.) were suspended in a mixture of toluene (10 mL/mmol), and the respective alcohol (10 mL/mmol, >100 equiv.). The reaction mixture was stirred at 40 °C for 16 hours. Subsequently, all volatiles were removed under reduced pressure on a rotary evaporator and the residue was subjected to column chromatography (silica gel, cyclohexane/ethyl acetate) to afford the desired product.

2.7. (*E*)-4,7-dimethoxy-11,12,17,18-tetrahydrotribenzo[*c,g,k*][1,2]diazacyclododecine (**2**)



Dimethoxy derivative **2** was synthesized according to the general procedure for the ortho alkoxylation using **1** (25 mg, 0.08 mmol, 1.0 equiv.), PIDA (77 mg, 0.24 mmol, 3.0 equiv.), Pd(OAc)<sub>2</sub> (7 mg, 0.03 mmol, 0.4 equiv.), methanol (0.8 g, 24 mmol, 300 equiv.), and toluene (1.0 mL). Purification by column chromatography (silica gel, cyclohexane:ethyl acetate; 100:0 → 70:30 (v/v)) afforded dimethoxy derivative **2** as a yellow powder in 43% yield (13 mg, 0.03 mmol).

$\text{C}_{24}\text{H}_{24}\text{N}_2\text{O}_2$  372.47 g mol<sup>-1</sup>

**R<sub>F</sub> value** (cyclohexane:ethyl acetate; 1:1 (v/v)) = 0.52

**<sup>1</sup>H NMR** (500 MHz, CDCl<sub>3</sub>, 298 K)  $\delta_{\text{H}}$  [ppm] = 2.92 (s, 4H, H-d), 3.00 (s, 4H, H-e), 3.96 (s, 6H, H-l), 6.98 (dd,  $J$  = 8.2, 1.2 Hz, 2H, H-i), 7.01 (dd,  $J$  = 7.5, 1.2 Hz, 2H, H-g), 7.24 – 7.17 (m, 2H, H-a), 7.32 – 7.25 (m, 2H, H-b), 7.32 (dd,  $J$  = 8.1, 7.6 Hz, 2H, H-h).

**<sup>13</sup>C NMR** (126 MHz, CDCl<sub>3</sub>, 298 K)  $\delta_{\text{C}}$  [ppm] = 20.71, 29.64, 36.10, 36.65, 77.49, 121.99, 126.48, 128.85, 130.15, 130.35, 137.37, 139.97, 143.78, 144.64, 169.22.

**HRMS** (ESI<sup>+</sup>-Orbitrap)  $m/z$  (relative intensity) = 373.1905 (100%, [M+H]<sup>+</sup>, calcd 373.1911), 395.172 (100%, [M+Na]<sup>+</sup>, calcd 395.1730).



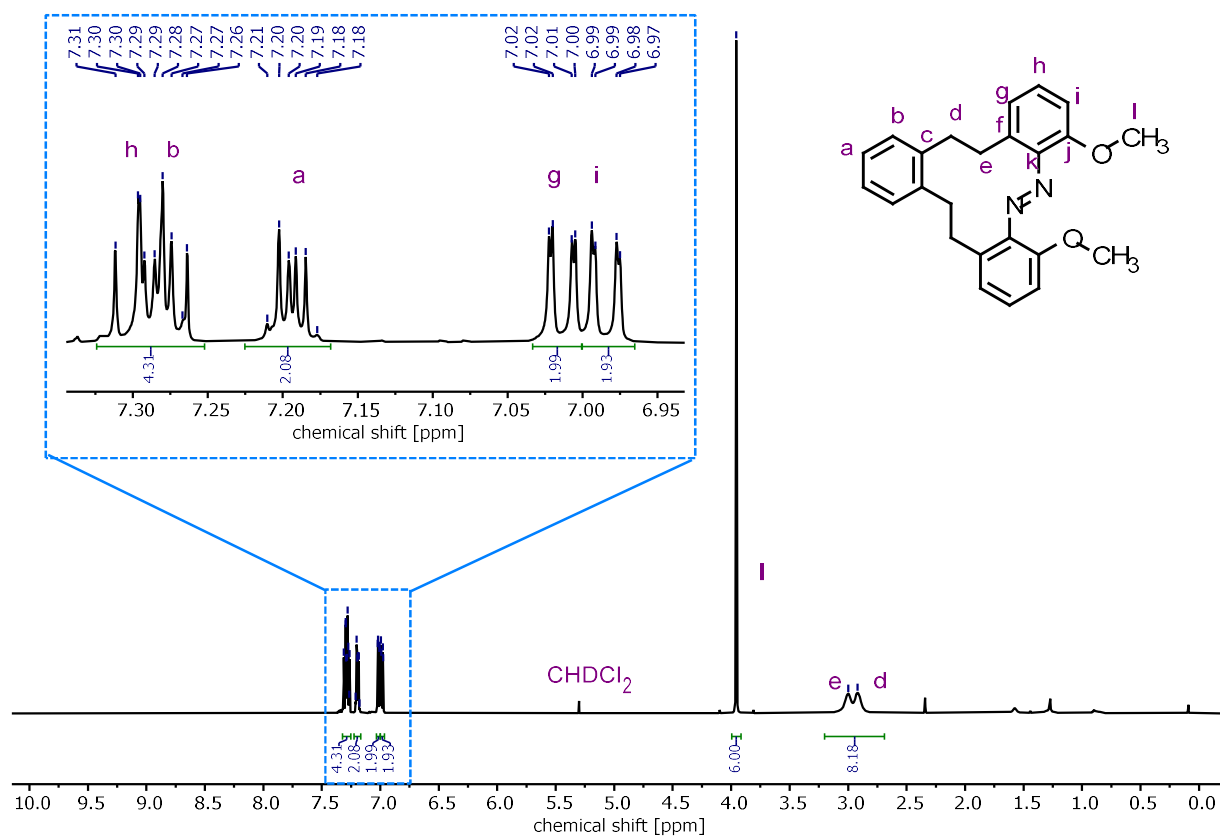


**Figure S9.** <sup>1</sup>H NMR spectrum (500 MHz, CD<sub>2</sub>Cl<sub>2</sub>, 298 K) of cyclic dimethoxy derivative **2**.

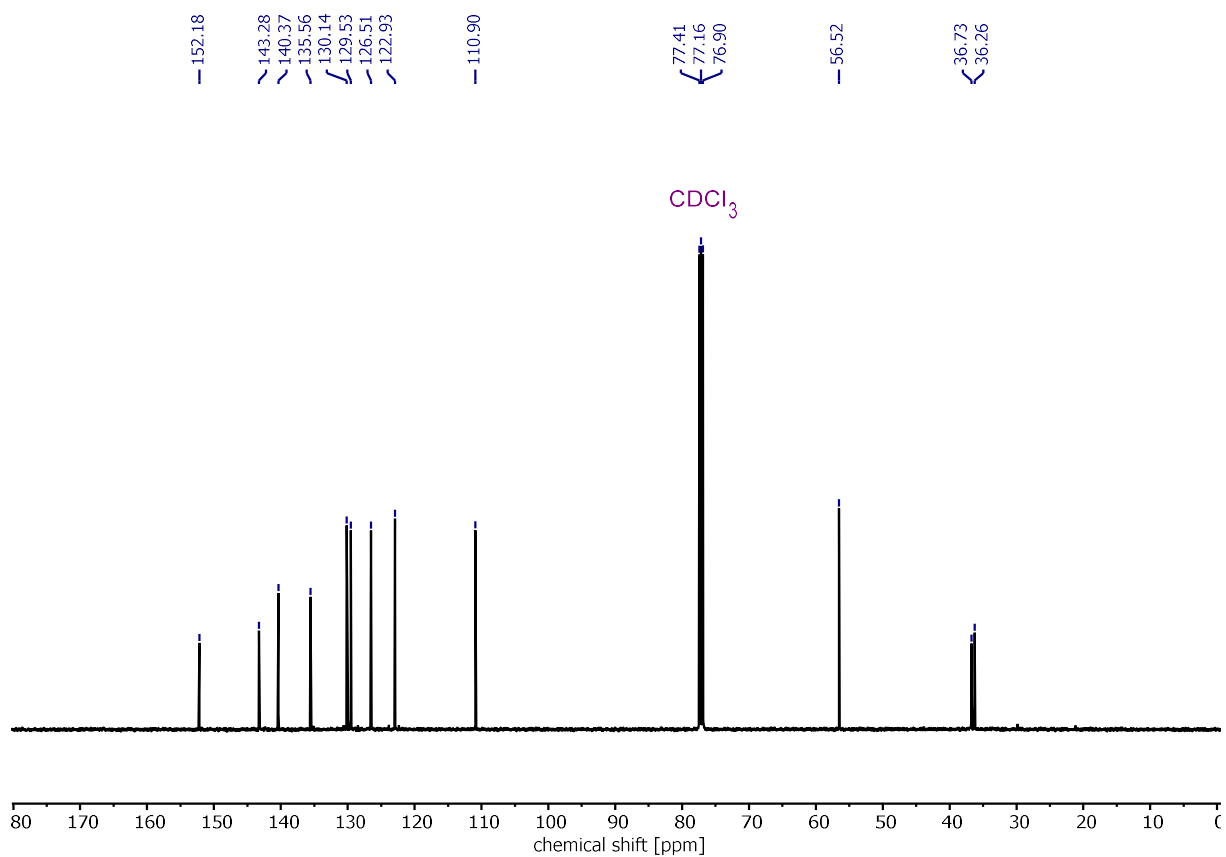
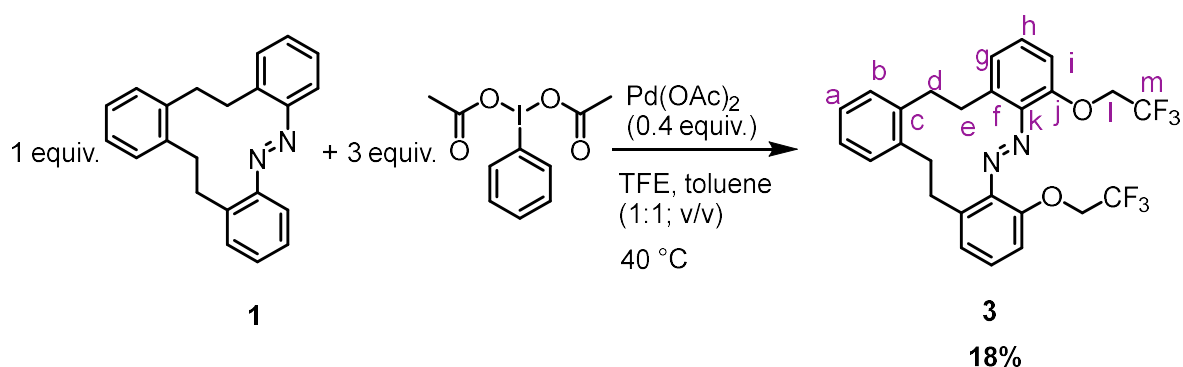


**Figure S10.** <sup>13</sup>C NMR spectrum (126 MHz, CDCl<sub>3</sub>, 298 K) of cyclic dimethoxy derivative **2**.

2.8. (*E*)-4,7-bis(2,2,2-trifluoroethoxy)-11,12,17,18-tetrahydrotribenzo[*c,g,k*][1,2]-diazacyclododecine (**3**)



Trifluoroethanoether derivative **3** was synthesized according to the general procedure for the ortho alkoxylation using **1** (30 mg, 0.10 mmol, 1.0 equiv.), PIDA (93 mg, 0.30 mmol, 3.0 equiv.), Pd(OAc)<sub>2</sub> (9 mg, 0.04 mmol, 0.4 equiv.), trifluoroethanol (TFE; 1.4 g, 14 mmol, 140 equiv.), and toluene (1.0 mL). Purification by column chromatography (silica gel, cyclohexane: ethyl acetate; 100:0 → 70:30 (v/v)) afforded trifluoroethanoether derivative **3** as an orange powder in 18% yield (9 mg, 0.02 mmol).

**C**<sub>26</sub>**H**<sub>22</sub>**F**<sub>6</sub>**N**<sub>2</sub>**O**<sub>2</sub>      508.46 g mol<sup>-1</sup>

**R**<sub>F</sub> (cyclohexane:ethyl acetate; 1:1 (v/v)) = 0.64

<sup>1</sup>H NMR (500 MHz, CD<sub>2</sub>Cl<sub>2</sub>, 298 K) δ<sub>H</sub> [ppm] = 2.94 (s, 4H, H-d), 3.05 (s, 4H, H-e), 4.47 (q, *J* = 8.6 Hz, 4H, H-l), 7.12 (dd, *J* = 8.2, 1.4 Hz, 2H, H-i), 7.14 – 7.20 (m, 2H, H-a), 7.18 (dd, *J* = 7.6, 1.4 Hz, 2H, H-g), 7.24 – 7.28 (m, 2H, H-b), 7.34 (dd, *J* = 8.2, 7.6 Hz, 2H, H-h).

<sup>13</sup>C NMR (126 MHz, CDCl<sub>3</sub>, 298 K) δ<sub>C</sub> [ppm] = 36.40, 36.92, 69.19 (q, *J* = 35.6 Hz), 117.20, 123.83 (q, *J* = 278.9 Hz), 126.42, 126.70, 130.22, 130.42, 136.97, 140.05, 144.28, 151.41.

<sup>19</sup>F NMR (471 MHz, CDCl<sub>3</sub>, 298 K) δ<sub>F</sub> [ppm] = -75.68 (t, *J* = 8.3 Hz).

HRMS (ESI<sup>+</sup>-Orbitrap): *m/z* (relative intensity) = 509.1657 (100%, [M+H]<sup>+</sup>, calcd 509.1658).

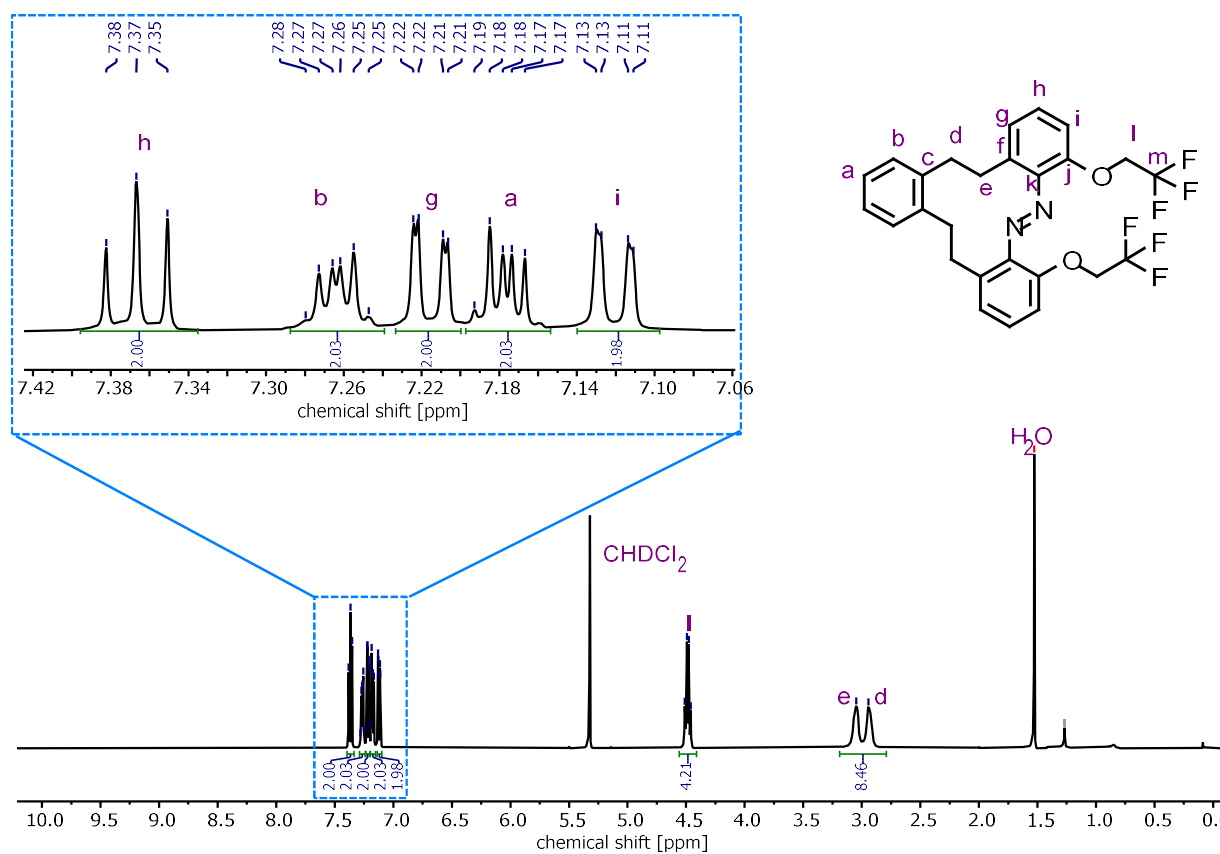


**Figure S11.**  $^1\text{H}$  NMR spectrum (500 MHz,  $\text{CD}_2\text{Cl}_2$ , 298 K) of cyclic dimethoxy derivative **3**.

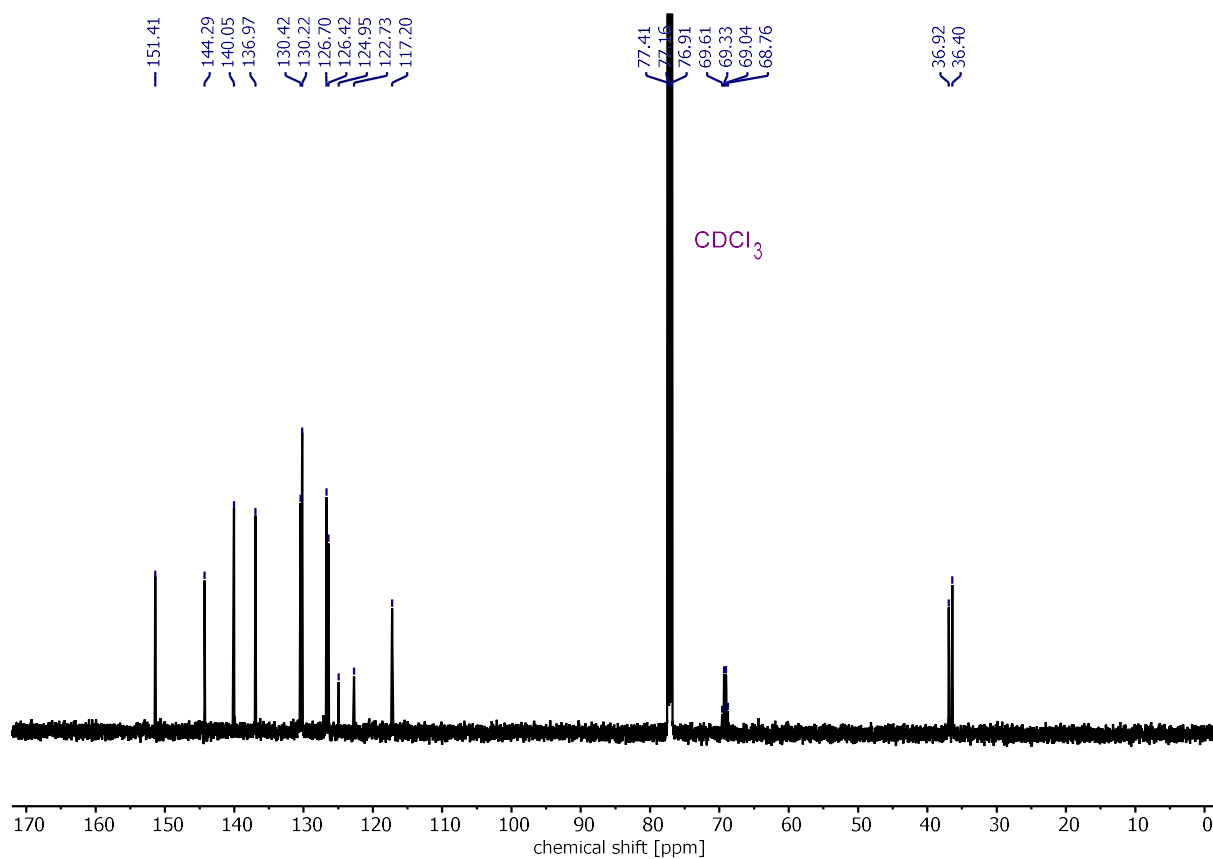


**Figure S12.**  $^{13}\text{C}$  NMR spectrum (126 MHz,  $\text{CDCl}_3$ , 298 K) of cyclic dimethoxy derivative **3**.

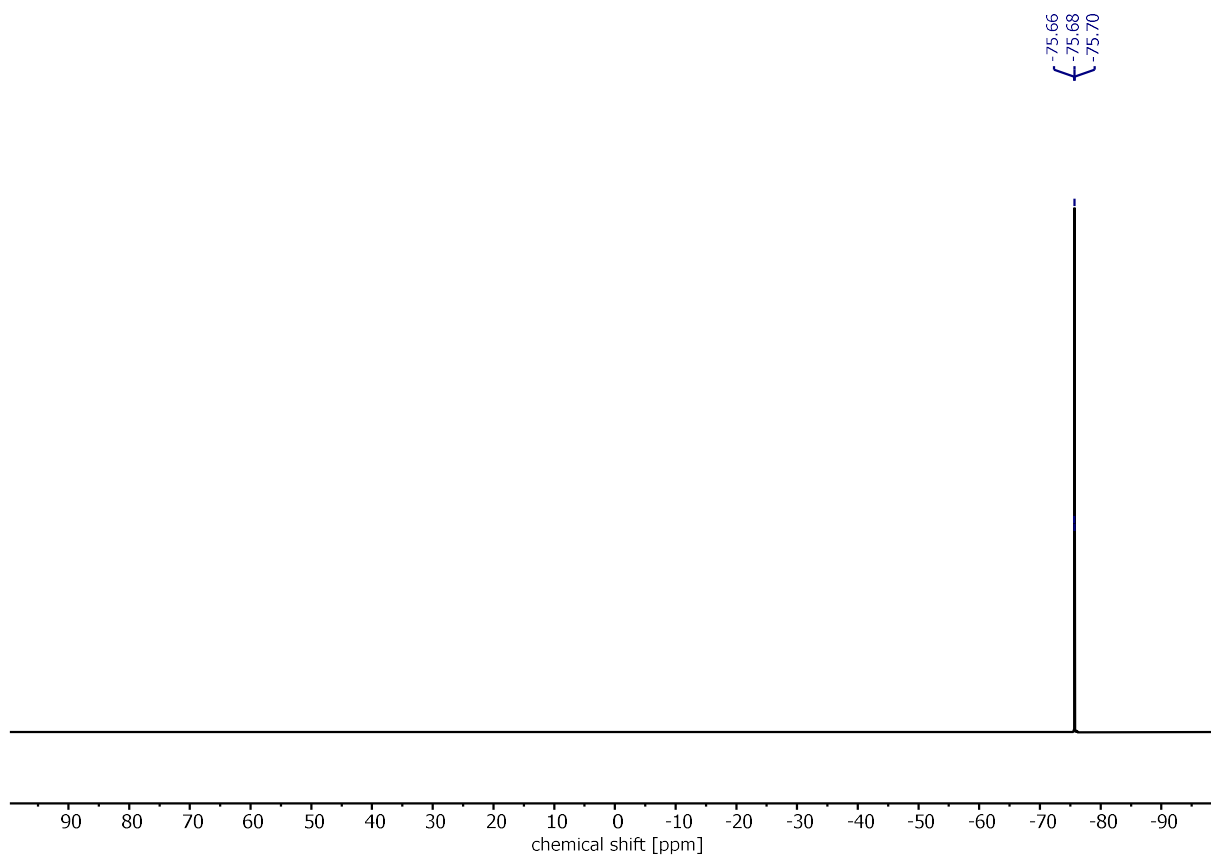
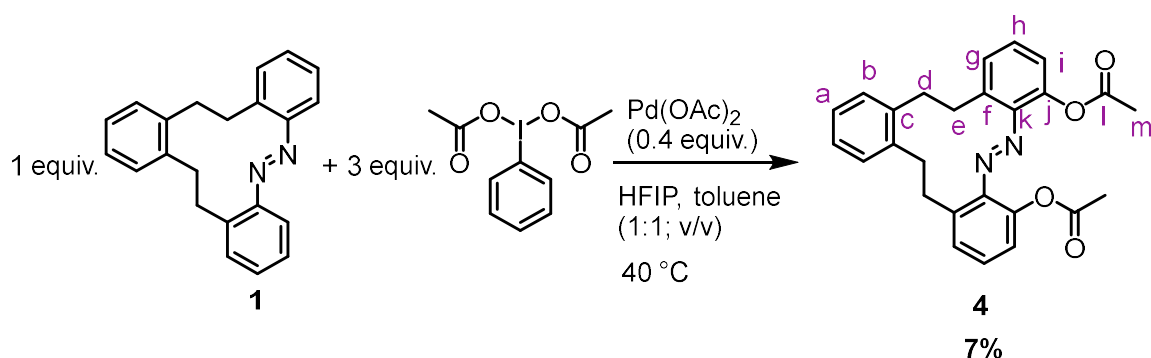


**Figure S13.**  $^{19}\text{F}$  NMR spectrum (471 MHz,  $\text{CDCl}_3$ , 298 K) of cyclic dimethoxy derivative **3**.

2.9. (*E*)-11,12,17,18-tetrahydrotribenzo[*c,g,k*][1,2]diazacyclododecine-4,7-diyl diacetate (**4**)



Acetyler ester derivative **4** was synthesized according to the general procedure for the ortho alkoxylation using **1** (30 mg, 0.10 mmol, 1.0 equiv.), PIDA (93 mg, 0.30 mmol, 3.0 equiv.), Pd(OAc)<sub>2</sub> (9 mg, 0.04 mmol, 0.4 equiv.), hexafluoroisopropanol (HFIP; 1.6 g, 10 mmol, 100 equiv.), and toluene (1.0 mL). Purification by column chromatography (silica gel, cyclohexane: ethyl acetate; 100:0 → 70:30 (v/v)) afforded only one compound which was the acetyler ester derivative **4** as a red powder in 7% yield (4 mg, 0.01 mmol).

The desired product of this reaction was the HFIP ether derivative. However, the only compound that could be isolated from the reaction mixture was the acetyler ester derivative **4**. The reaction was carried out three times with the same result.



$R_F$  (cyclohexane: ethyl acetate; 1:1 (v/v)) = 0.62.

<sup>1</sup>H NMR (500 MHz, CD<sub>2</sub>Cl<sub>2</sub>, 298 K)  $\delta_H$  [ppm] = 2.33 (s, 6H, H-m), 2.98 (s, 4H, H-d), 3.08 (s, 4H, H-e), 7.09 (dd,  $J$  = 8.0, 1.5 Hz, 2H, H-i), 7.20 – 7.14 (m, 2H, H-a), 7.27 – 7.23 (m, 2H, H-b), 7.34 (dd,  $J$  = 7.7, 1.5 Hz, 2H, H-g), 7.41 (t,  $J$  = 7.8 Hz, 2H, H-h).

<sup>13</sup>C NMR (126 MHz, CD<sub>2</sub>Cl<sub>2</sub>, 298 K)  $\delta_C$  [ppm] = 20.71, 29.64, 36.10, 36.65, 77.49, 121.99, 126.48, 128.85, 130.15, 130.35, 137.37, 139.97, 143.78, 144.64, 169.22.

HRMS (ESI<sup>+</sup>-Orbitrap)  $m/z$  (relative intensity) = 429.1809 (100%, [M+H]<sup>+</sup>, calcd 429.1809), 387.170 (53%, [M+H-Ac]<sup>+</sup>, calcd 387.1703).

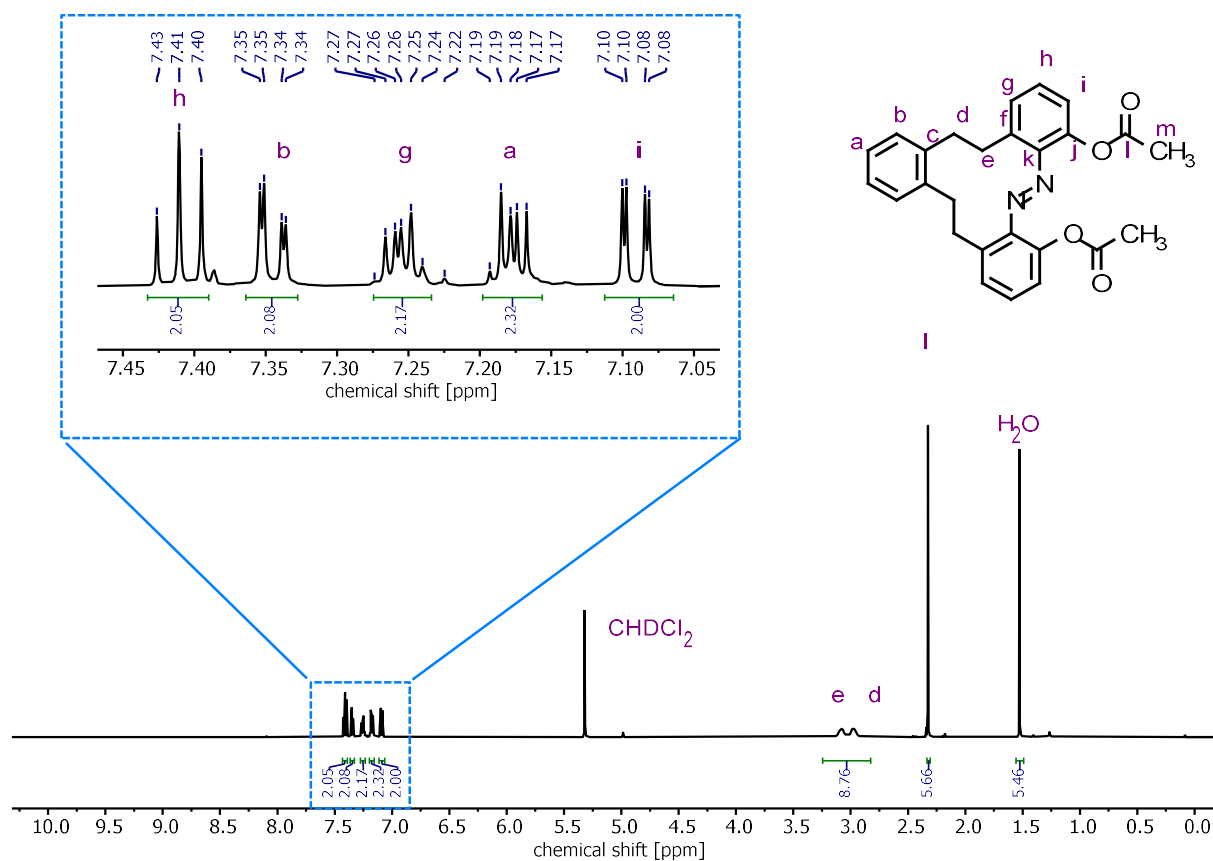


**Figure S14.**  $^1\text{H}$  NMR spectrum (500 MHz,  $\text{CD}_2\text{Cl}_2$ , 298 K) of cyclic dimethoxy derivative **4**.

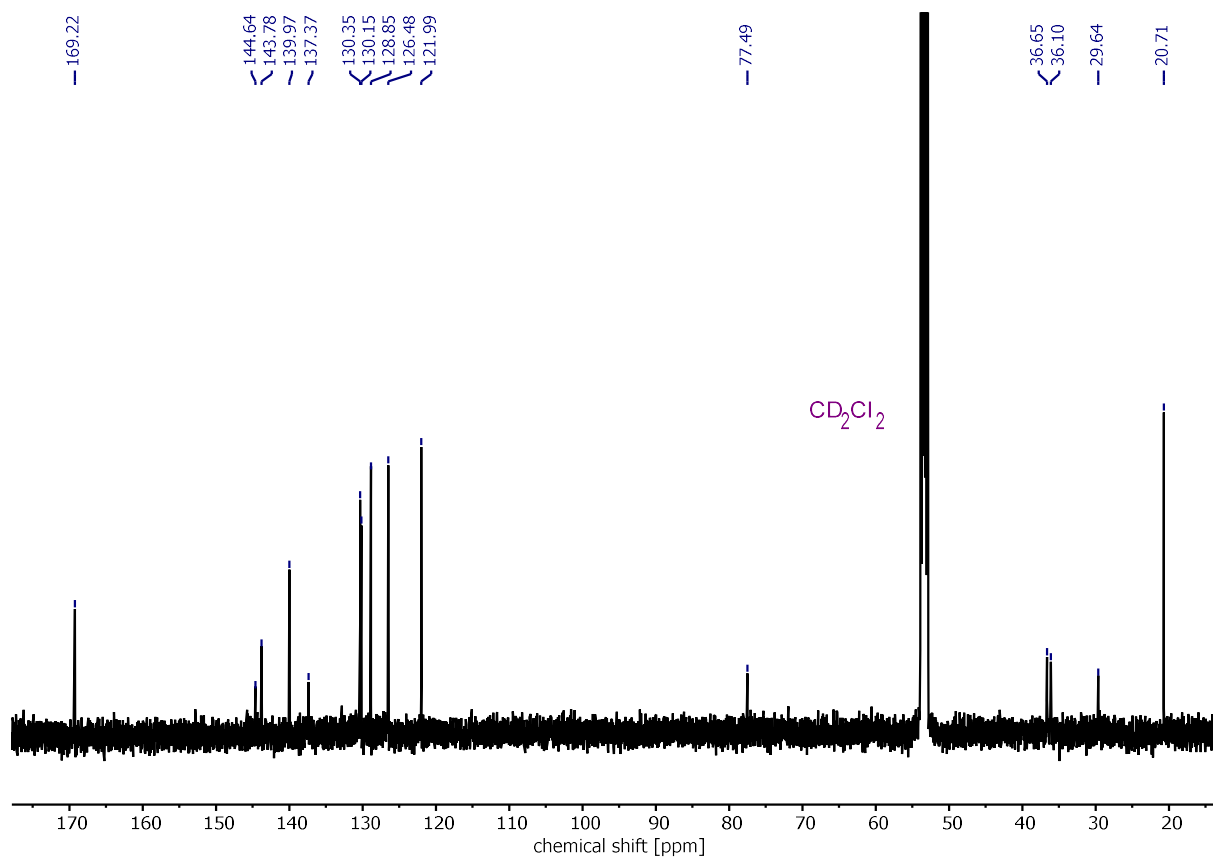
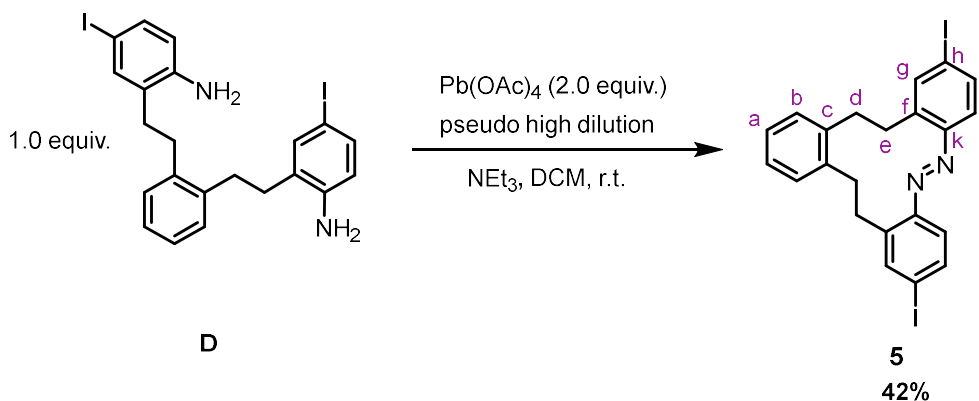


**Figure S15.**  $^{13}\text{C}$  NMR spectrum (126 MHz,  $\text{CDCl}_3$ , 298 K) of cyclic dimethoxy derivative **3**.

2.10. (*E*)-2,9-diiodo-11,12,17,18-tetrahydrotribenzo[*c,g,k*][1,2]diazacyclododecine (**5**)



A three-necked flask was equipped with two 250 mL dropping funnels. One funnel was loaded with a solution of diiodide **D** (100 mg, 0.316 mmol, 1.00 equiv., 3 mmol/L), and TEA (1 mL) in DCM (100 mL) and the other dropping funnel was loaded with a solution of lead(IV) acetate (280 mg, 0.632 mmol, 2.00 equiv., 6 mmol/L) in DCM (100 mL). Both solutions were added dropwise into DCM (250 mL) within 30 min. After complete addition, the solution was stirred at room temperature for 30 min. Afterwards the solution was concentrated under reduced pressure. The residue was filtered over a silica plug (5 cm diameter, 5 cm height) with cyclohexane. Diiodinated macrocyclic azobenzene **5** was obtained as an orange solid (66 mg, 116  $\mu\text{mol}$ , 42%).

$\text{C}_{22}\text{H}_{18}\text{I}_2\text{N}_2$                       564.21  $\text{g mol}^{-1}$

**R<sub>F</sub> value** (cyclohexane:ethyl acetate; 8:2 (v/v)) = 0.67

**<sup>1</sup>H NMR** (500 MHz,  $\text{CD}_2\text{Cl}_2$ , 298 K):  $\delta_{\text{H}}$  [ppm] = 2.57 – 3.60 (m, 6H, H-d,e), 7.16 – 7.22 (m, 2H, H-a), 7.24 – 7.31 (m, 2H, H-b), 7.66 (d,  $J$  = 8.3 Hz, 2H, H-j), 7.79 (dd,  $J$  = 8.4, 2.0 Hz, 2H, H-i), 7.84 (d,  $J$  = 2.0 Hz, 2H, H-g).

**<sup>13</sup>C NMR** (126 MHz,  $\text{CD}_2\text{Cl}_2$ , 298 K):  $\delta_{\text{C}}$  [ppm] = 36.27, 37.55, 97.94, 126.07, 126.84, 130.54, 136.88, 139.93, 140.25, 140.84, 150.49.

**HRMS** (ESI<sup>+</sup>-Orbitrap):  $m/z$  (relative intensity) = 564.9632 (100%,  $[\text{M}+\text{H}]^+$ , calcd 564.9626).

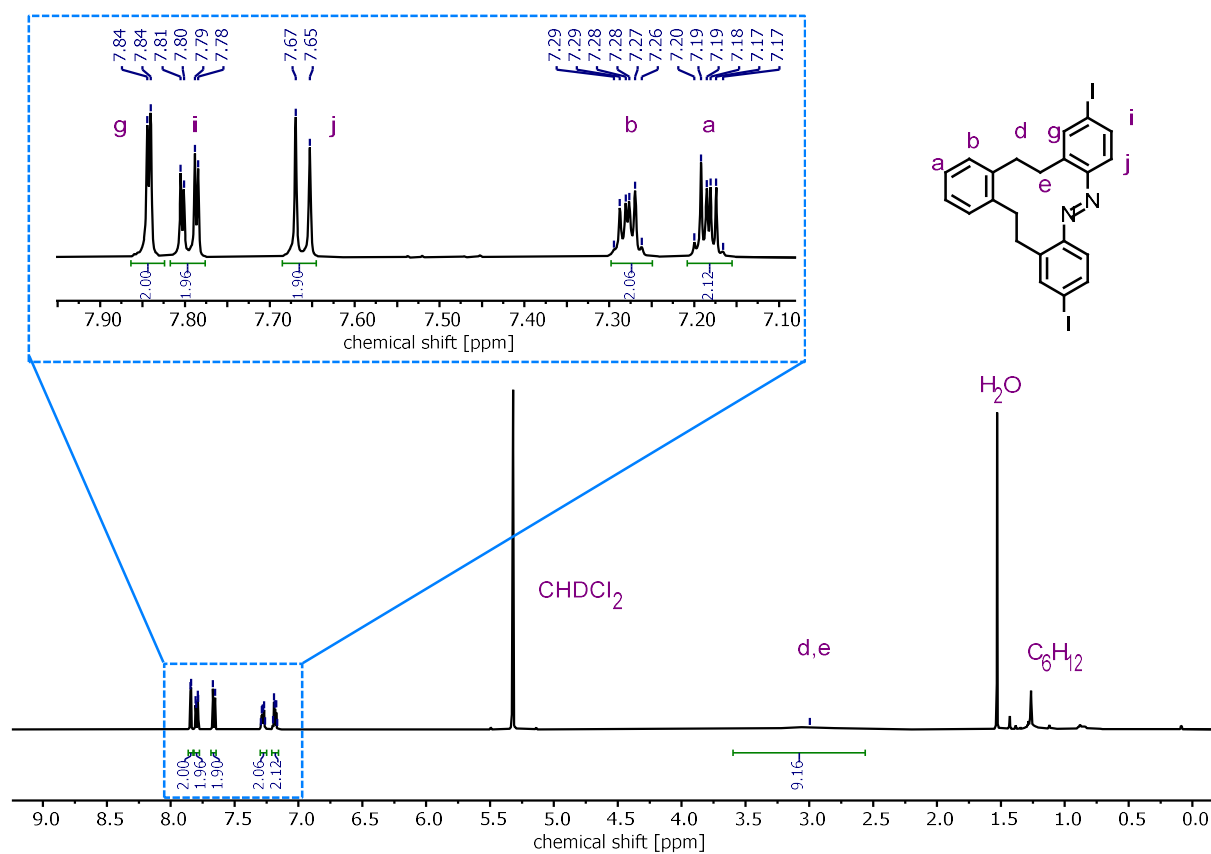


Figure S16.  $^1\text{H}$  NMR spectrum (500 MHz,  $\text{CD}_2\text{Cl}_2$ , 298 K) of cyclic azobenzene **5**.

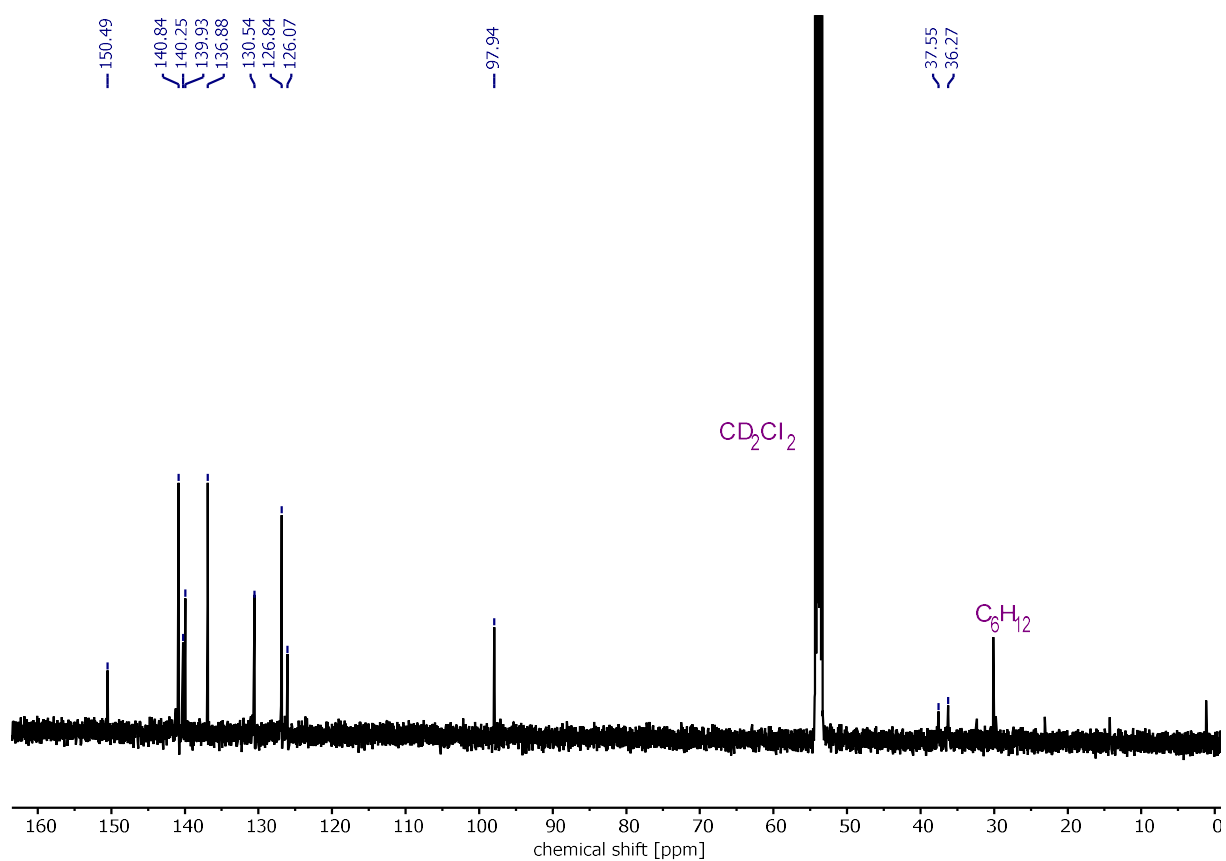
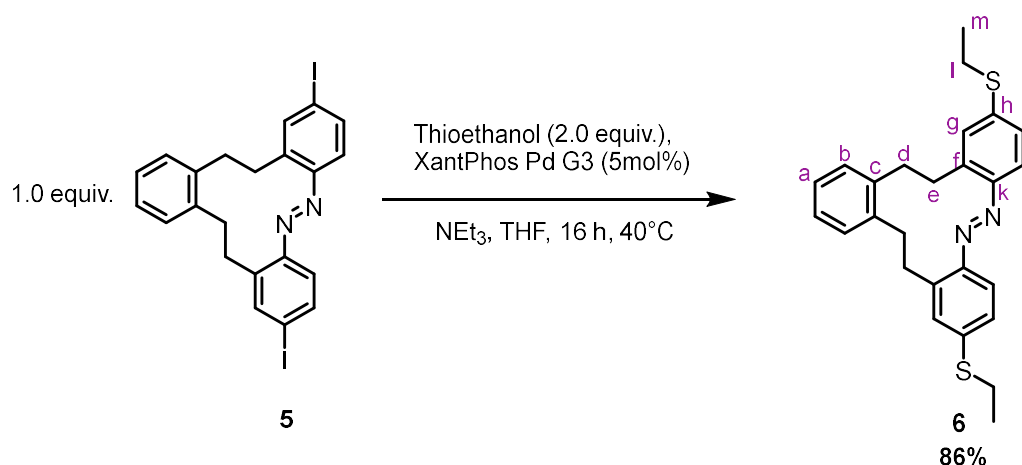


Figure S17.  $^{13}\text{C}$  NMR spectrum (126 MHz,  $\text{CD}_2\text{Cl}_2$ , 298 K) of cyclic azobenzene **5**.



2.11. (*E*)-2,9-bis(ethylthio)-11,12,17,18-tetrahydrotribenzo[*c,g,k*][1,2]diazacyclododecine (**6**)



A flame dried schlenk flask was loaded with diiodinated macrocyclic azobenzene **5** (30.0 mg, 53.2  $\mu\text{mol}$ , 1.00 equiv.), thioethanol (9.0 mg, 142  $\mu\text{mol}$  2.00 equiv.), and XantPhos Pd G3 (1.5 mg, 1.44  $\mu\text{mol}$ , 0.02 equiv.) and vacuum was applied for 15 min. Meanwhile dry THF (10 mL) was degassed by bubbling Ar through. Then the flask was filled with a Ar atmosphere and the solvent was added, followed by dry  $\text{NEt}_3$  (1 mL). The reaction was stirred at 40  $^\circ\text{C}$  for 16 h. After cooling to room temperature, the reaction mixture was diluted with EtOAc (10 mL), washed with aq. 1 M HCl (10 mL) and saturated aqueous NaCl solution (10 mL), and the aqueous phase was extracted with EtOAc (3x 50 mL). The combined organic layers were dried over  $\text{MgSO}_4$ , filtered, and concentrated in under reduced pressure at a rotary evaporator. Column chromatography (cyclohexane) afforded the desired compound **6** (20 mg, 53  $\mu\text{mol}$ , 86%).

$\text{C}_{26}\text{H}_{28}\text{N}_2\text{S}_2$  432.17  $\text{g mol}^{-1}$

**R<sub>F</sub> value** (cyclohexane:ethyl acetate; 8:2 (v/v)) = 0.75

**<sup>1</sup>H NMR** (400 MHz,  $\text{CD}_2\text{Cl}_2$ , 298 K)  $\delta_{\text{H}}$  [ppm] = 1.41 (t,  $J$  = 7.4 Hz, 6H, H-l), 2.54 – 3.55 (m, 8H, H-d,e), 3.09 (q,  $J$  = 7.4 Hz, 4H, H-m), 7.15 – 7.22 (m, 2H, H-a), 7.25 – 7.35 (m, 6H, H-b,g,i), 7.88 (d,  $J$  = 8.9 Hz, 2H, H-j).

**<sup>13</sup>C NMR** (126 MHz,  $\text{CD}_2\text{Cl}_2$ , 298 K)  $\delta_{\text{C}}$  [ppm] = 8.78, 14.39, 26.91, 46.16, 124.93, 125.71, 126.66, 129.92, 130.49, 138.55, 140.66, 141.28, 148.63.

**HRMS** (ESI<sup>+</sup>-Orbitrap):  $m/z$  (relative intensity) = 433.1764 (100%,  $[\text{M}+\text{H}]^+$ , calcd 433.1767).

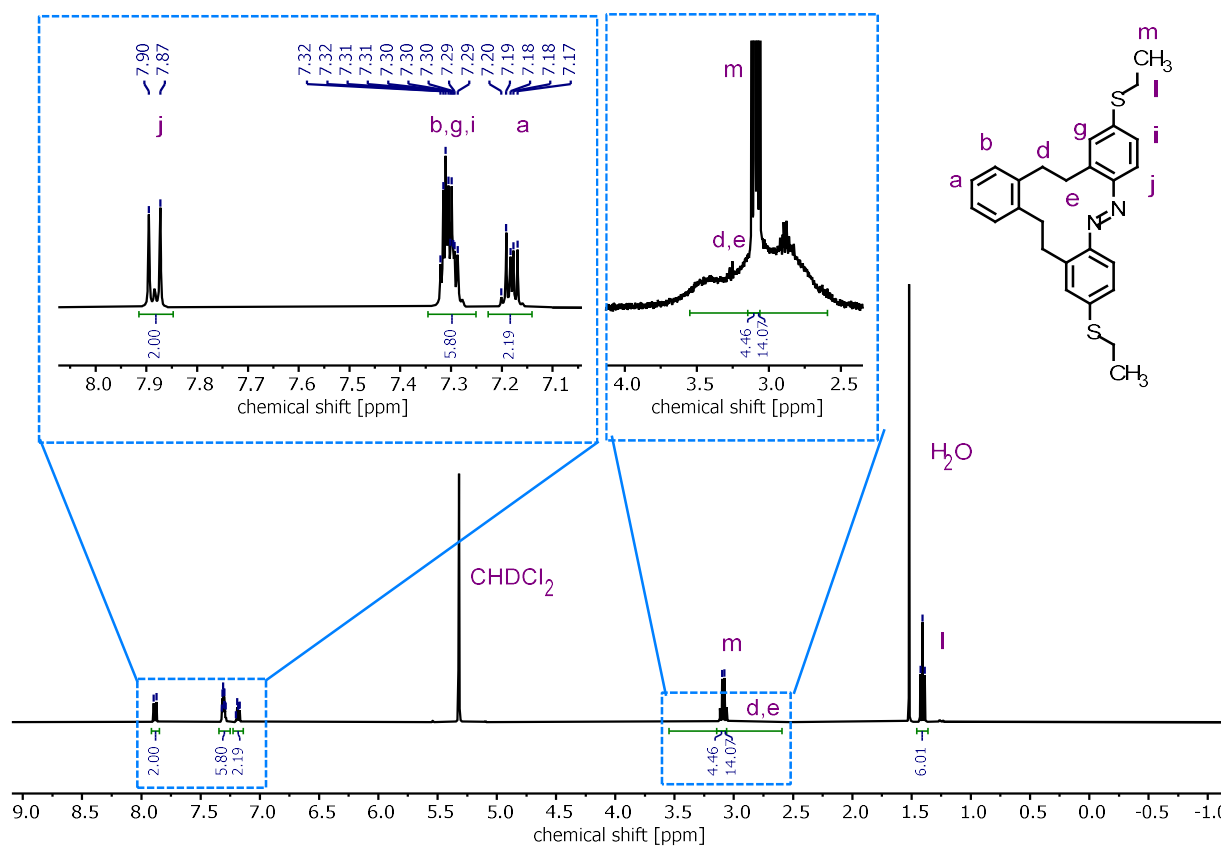


**Figure S18.** <sup>1</sup>H NMR spectrum (400 MHz, CD<sub>2</sub>Cl<sub>2</sub>, 298 K) of thioether derivative **6**.

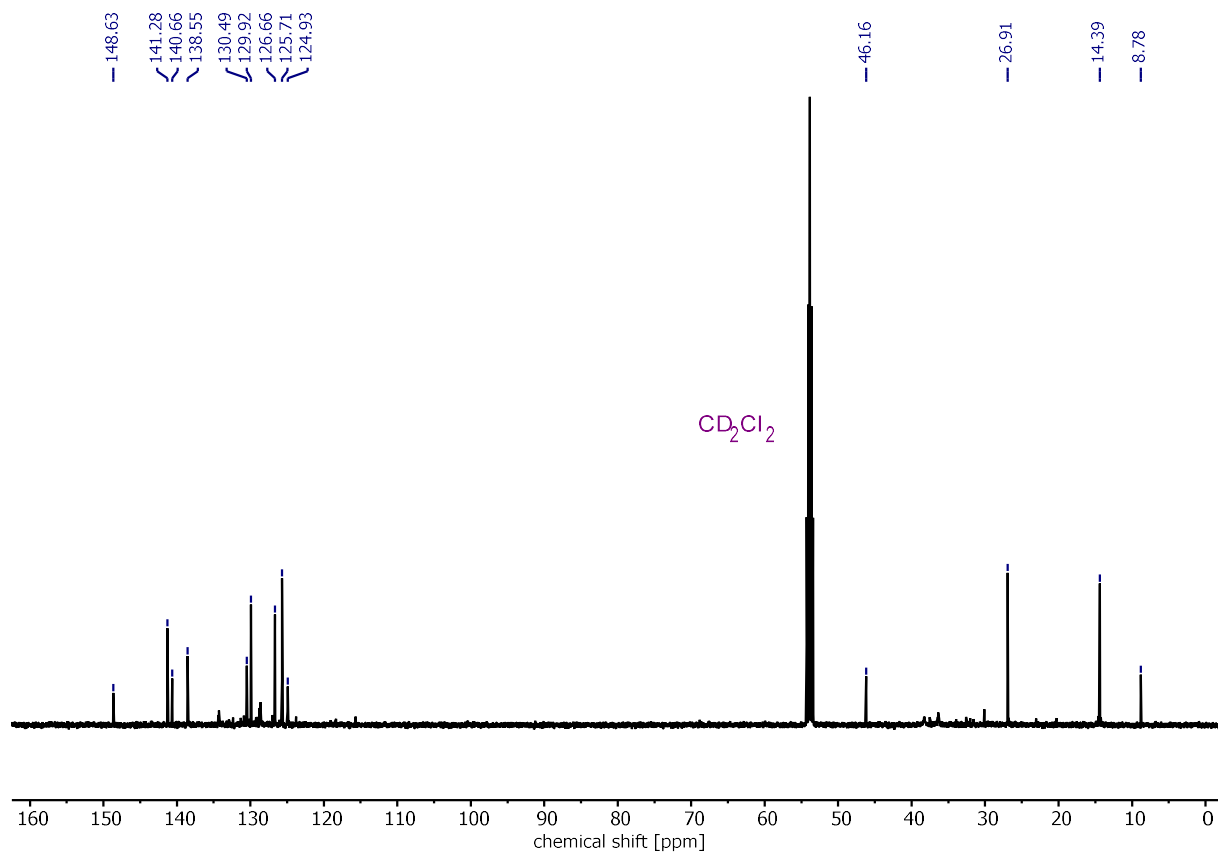
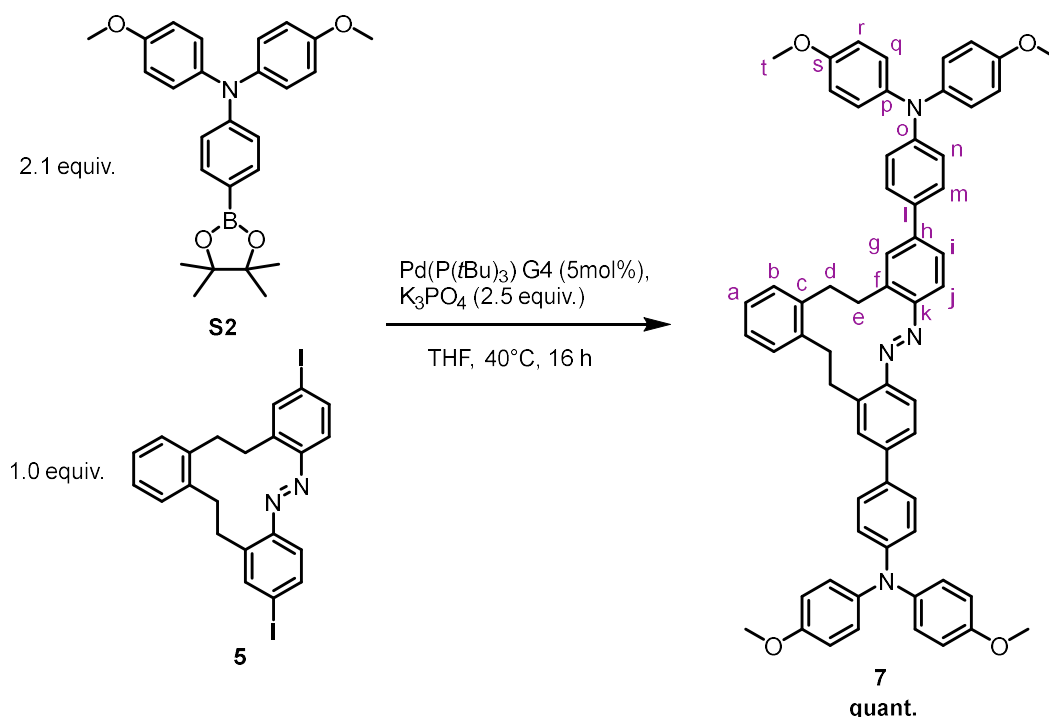


**Figure S19.** <sup>13</sup>C NMR spectrum (126 MHz, CD<sub>2</sub>Cl<sub>2</sub>, 298 K) of thioether derivative **6**.

2.12. (*E*)-4,4'-(11,12,17,18-tetrahydrotribenzo[*c,g,k*][1,2]diazacyclododecine-2,9-diyl)bis(*N,N*-bis(4-methoxyphenyl)aniline) (**7**)



A flame dried Schlenk flask was loaded with diiodinated macrocyclic azobenzene **5** (24 mg, 42.54  $\mu\text{mol}$ , 1.00 equiv.), boronic acid pinacolester **S2** (38.5 mg, 89.5  $\mu\text{mol}$ , 2.10 equiv.), and Pd(P(*t*Bu)<sub>3</sub>) G4 (1.25 mg, 2.13  $\mu\text{mol}$ , 0.05 equiv.) and vacuum was applied for 15 min. Meanwhile dry THF (10 mL) was degassed by bubbling Ar through. Then the flask was filled with a Ar atmosphere and the solvent was added, followed by K<sub>3</sub>PO<sub>4</sub> (22.5 mg, 106  $\mu\text{mol}$ , 2.50 equiv.). The reaction was stirred at the 40 °C for 16 h. After cooling to room temperature, the reaction mixture was diluted with EtOAc (10 mL), washed with aq. 1 M HCl (10 mL) and saturated aqueous NaCl solution (10 mL), and the aqueous phase was extracted with EtOAc (3x 50 mL). The combined organic layers were dried over MgSO<sub>4</sub>, filtered, and concentrated in under reduced pressure at a rotary evaporator. Column chromatography (cyclohexane:ethylacetate:1:1) afforded the desired product **7** (39 mg, 42  $\mu\text{mol}$ , quant.).

C<sub>62</sub>H<sub>54</sub>N<sub>4</sub>O<sub>4</sub>            919.14 g mol<sup>-1</sup>

**R<sub>F</sub> value** (cyclohexane:ethyl acetate; 8:2 (v/v)) = 0.48

<sup>1</sup>H NMR (700 MHz, CD<sub>2</sub>Cl<sub>2</sub>, 298 K)  $\delta_{\text{H}}$  [ppm] = 3.81 (s, 12H, H-t), 6.87 – 6.89 (m, 8H, H-r), 6.99 – 7.01 (m, 4H, H-n), 7.10 – 7.12 (m, 8H, H-q), 7.17 – 7.20 (m, 2H, H-a), 7.33 (dd, *J* = 5.5, 3.4 Hz, 2H, H-b), 7.55 – 7.59 (m, 4H, H-m), 7.63 – 7.66 (m, 4H, H-g,i), 8.02 (d, *J* = 8.6 Hz, 2H, H-j).

**<sup>13</sup>C NMR** (176 MHz, CD<sub>2</sub>Cl<sub>2</sub>, 298 K) δ<sub>C</sub> [ppm] = 24.62, 26.91, 55.45, 108.48, 114.72, 118.72, 120.07, 124.71, 126.22, 126.43, 126.93, 127.48, 129.03, 131.32, 138.10, 140.54, 142.56, 148.90, 156.32.

**HRMS** (ESI<sup>+</sup>-Orbitrap): *m/z* (relative intensity) = 918.4142 (100%, [M+H]<sup>+</sup>, 918.4140).

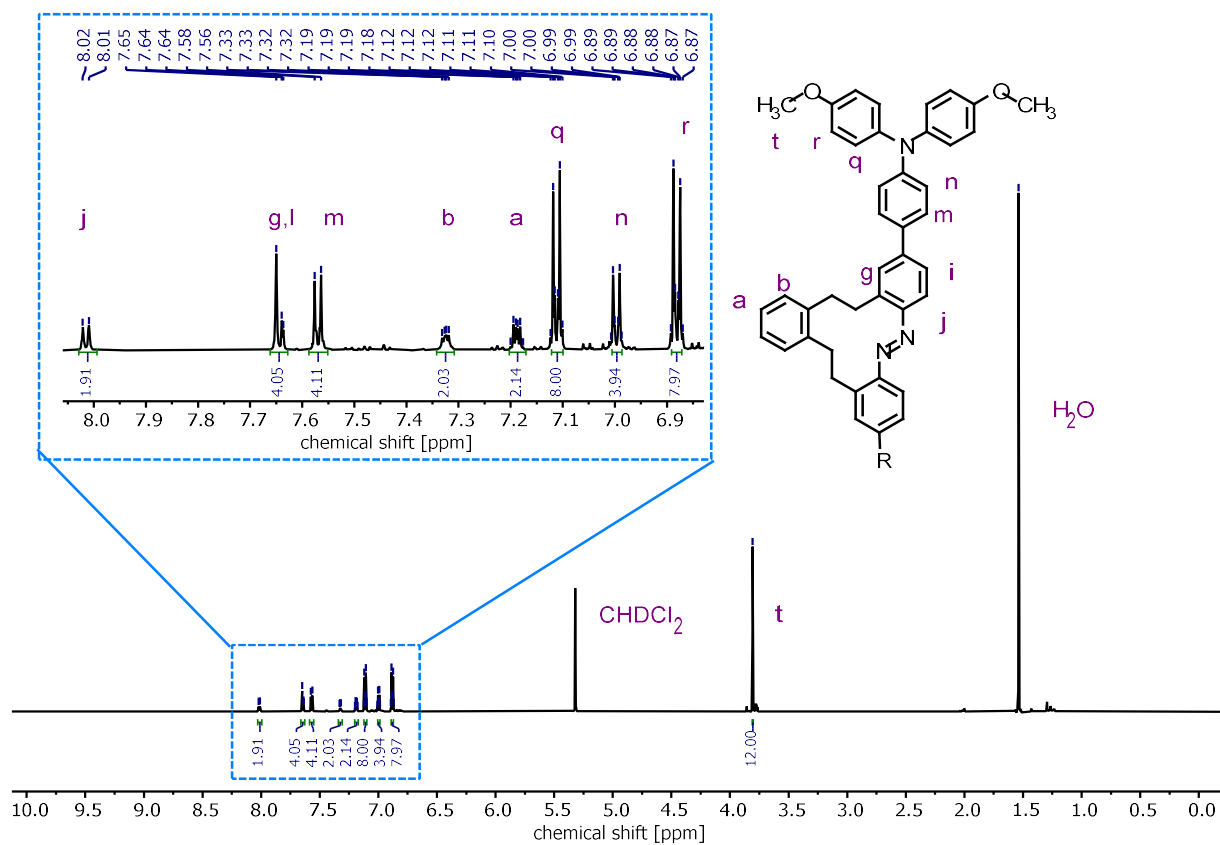


**Figure S20.**  $^1\text{H}$  NMR spectrum (700 MHz,  $\text{CD}_2\text{Cl}_2$ , 298 K) of cyclic azobenzene **7**.

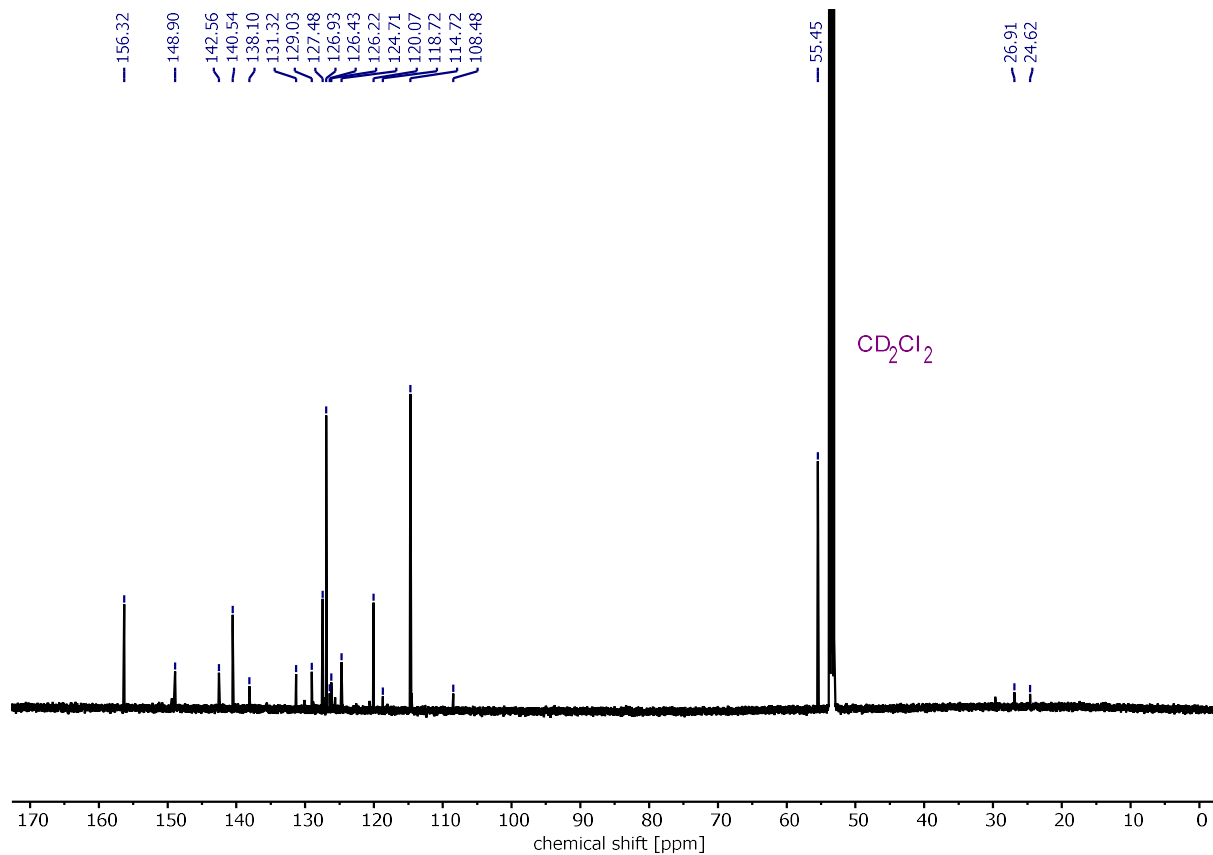


**Figure S21.**  $^{13}\text{C}$  NMR spectrum (176 MHz,  $\text{CD}_2\text{Cl}_2$ , 298 K) of cyclic azobenzene **7**.

### 3. Photophysical characterization

#### 3.1. General procedures for the illumination of different types of samples

Irradiation of single samples. Single samples in amberised vials or on 96-well plates were irradiated from a distance of 2 cm using a collimator that was connected to the respective light sources using a 60 cm long quartz glass fibre. The collimator gave a light spot with an approximate diameter of 4 cm.



**Figure S22.** Irradiation setup with a collimator connected to the fibre collimated light source showing an evenly irradiated circle with a diameter of 4 cm. Samples were placed 2 cm under the collimator.

**Irradiation of 96-well plates.** The filled 96-well plates (UV grade PP) were irradiated using a non-terminated optical fibre attached to a custom 3d printed box (136 mm × 146 mm × 96 mm) designed to achieve even and reproducible irradiation by placing the optical fibre exactly 13.0 cm above the centre of the well plate. Irradiation times to reach the PSS were usually longer with this setup since a larger area was illuminated. A quartz glass plate of appropriate dimensions was used as a lid for the 96-well plate, being fixed to the well plate using Teflon tape to reduce evaporation.

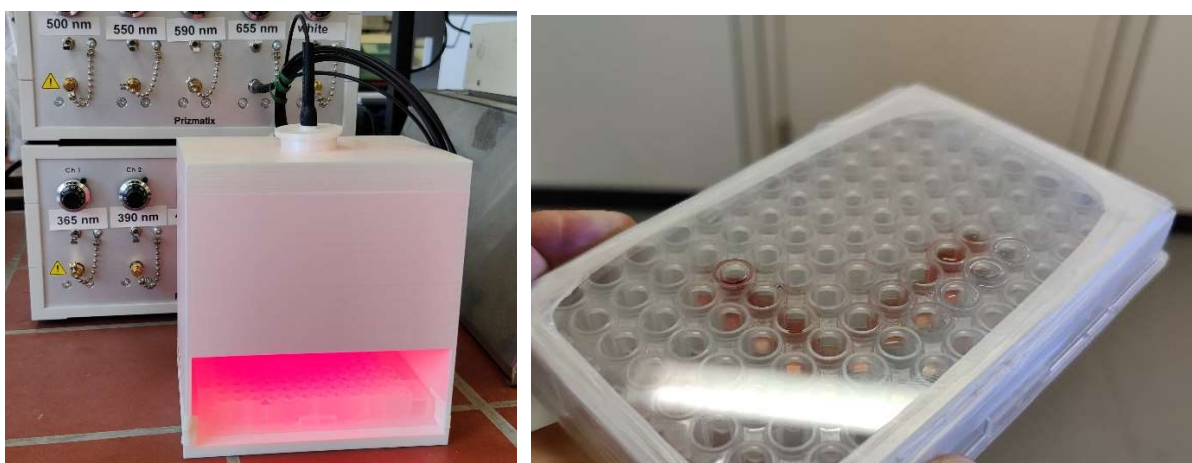


**Figure S23.** 3D printed chamber (136 mm × 146 mm × 96 mm) for even and reproducible irradiation of 96-well plates (left) and 96-well plate with quartz glass lid and Teflon tape seal (right).

### 3.2. NMR measurements of irradiated samples

***In-situ* illumination.** The NMR sample was fitted with an insert tube made from quartz glass and a quartz glass optical fibre was pushed down into the insert. The end of this fibre was non terminated, and the exposed surface had been roughened to ensure even and omnidirectional illumination. This construction was lowered into the NMR device using an aluminium rod to avoid damage to the fibre. The other end of the optical fibre was connected to the light source so the sample could be irradiated inside the spectrometer.<sup>3</sup>



**Figure S24.** NMR sample with quartz glass insert and optical fibre for *in-situ* illumination during NMR experiments.

***Ex-situ* illumination.** The sample was irradiated in an amberised vial (2 mL volume) using the setup shown in **Figure S22**, transferred into an amberised NMR tube in a dark room, and shielded from ambient light by aluminium foil until placed in the NMR autosampler.<sup>1,4</sup>

**Determination of the photo stationary state (PSS) by <sup>1</sup>H NMR spectroscopy.** Two signals corresponding to the same proton were integrated.  $PSS^{NMR}$  corresponds to that integral ratio. Well separated and resolved signals were chosen to ensure the most accurate results. Usually, the signal of the proton in the ortho-position to the azo bridge was chosen.<sup>1,4</sup>

### 3.2.1. Cyclic azobenzene 1

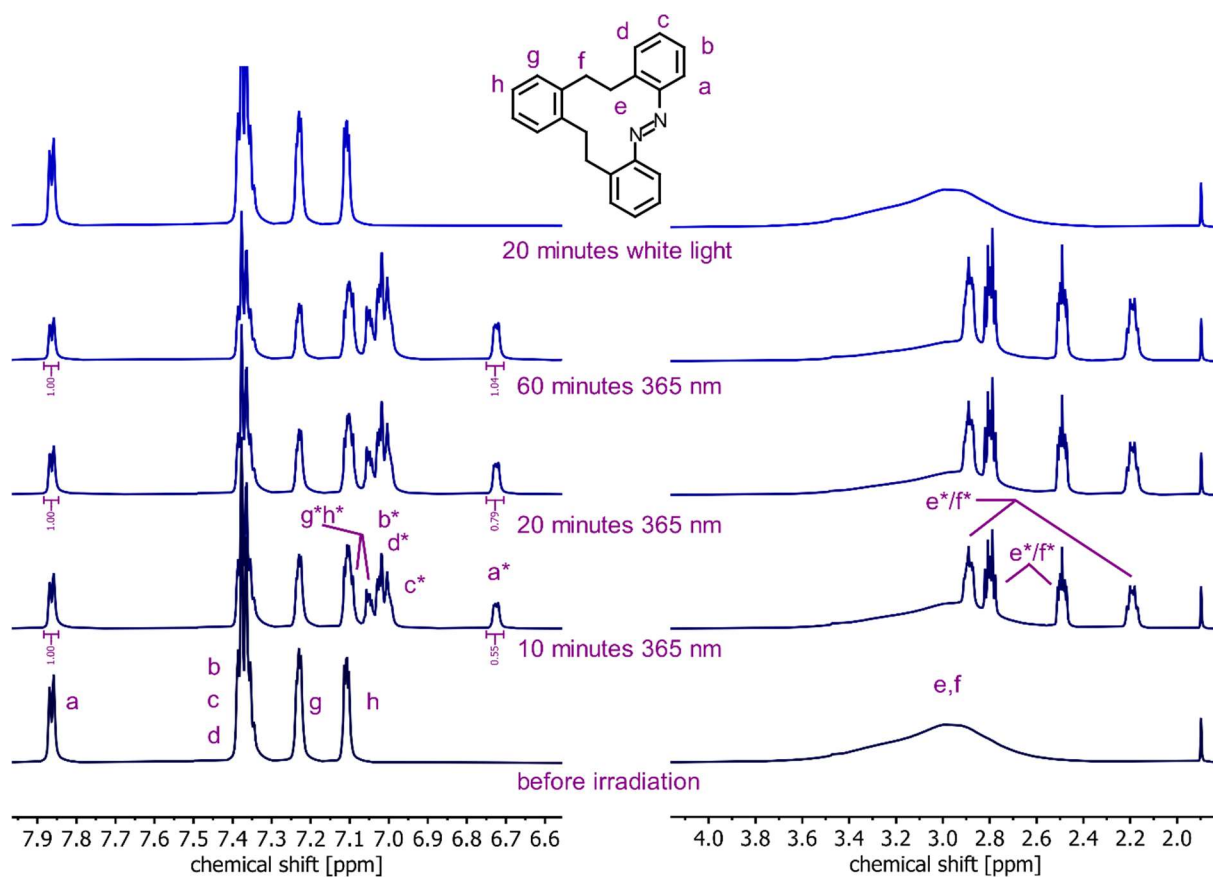


**Figure S25.** Partial  $^1\text{H}$  NMR spectra (700 MHz,  $\text{CD}_2\text{Cl}_2$ , 3 mM, 298 K) of cyclic azobenzene **1** during *in-situ* illumination experiments. Integration of the ortho  $\text{H}_a$  signals gives 0% **Z-1** before irradiation and after irradiation with white light (20 min) and 34%, 42%, and 51% **Z-1** after irradiation with 365 nm light for 10, 20, and 60 min, respectively.



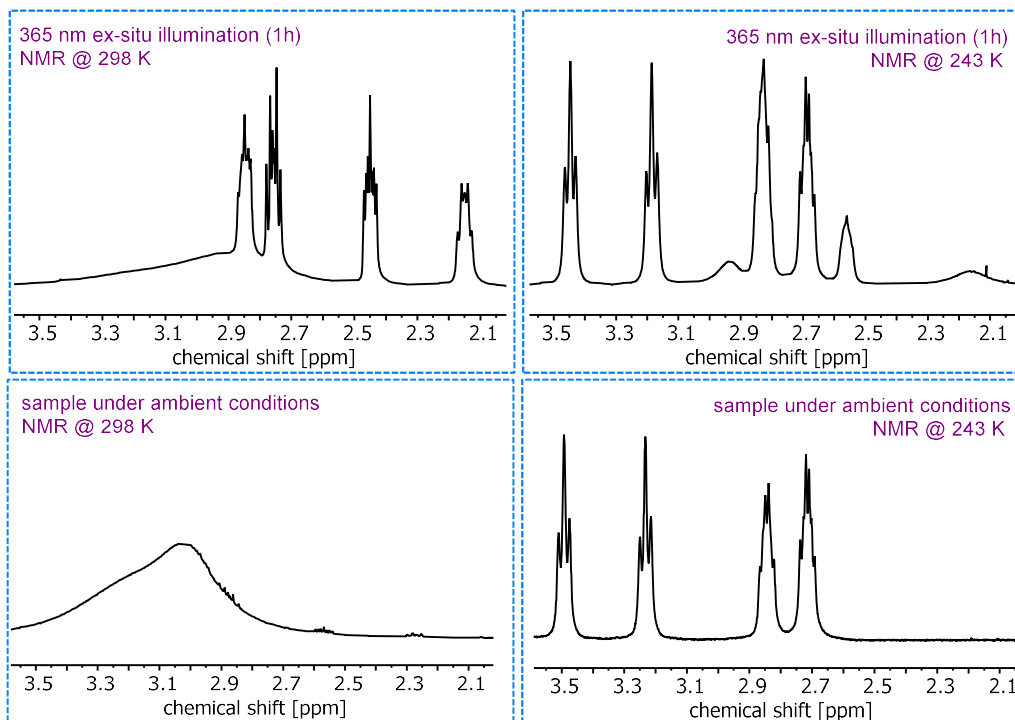


**Figure S26.** Partial  $^1\text{H}$  NMR spectra (500 MHz,  $\text{CD}_2\text{Cl}_2$ ) of cyclic azobenzene **1** showing  $\text{H}_e$  and  $\text{H}_f$  proton signals at 298 K (left) and 243 K (right) at ambient conditions (bottom) and after *ex-situ* illumination (365 nm, 60 min; top).

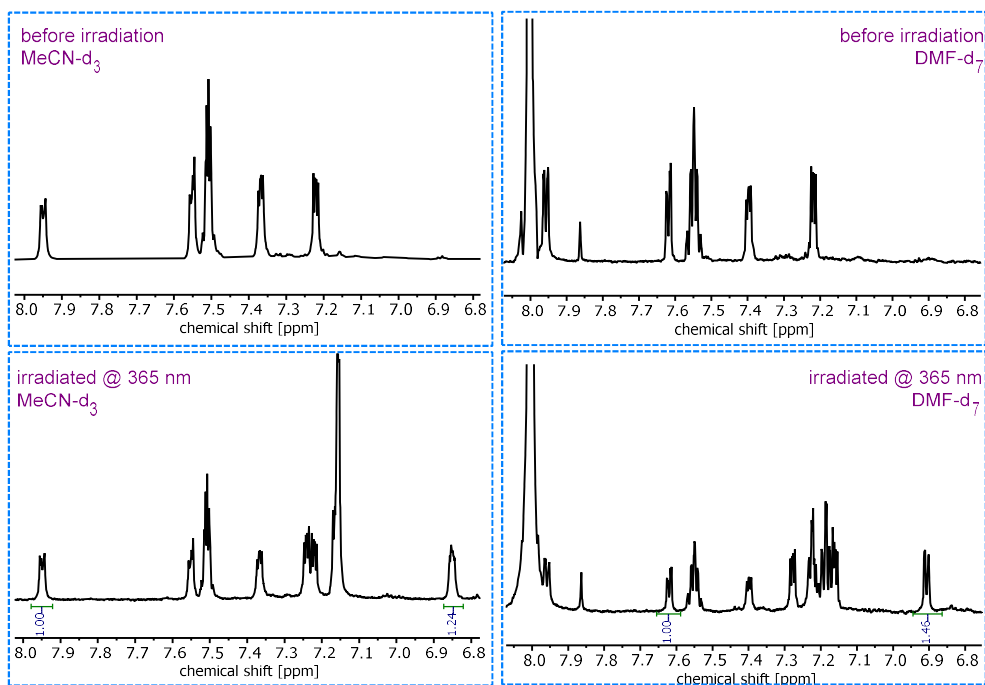


**Figure S27.** Partial  $^1\text{H}$  NMR spectra (700 MHz, 298 K) in  $\text{CD}_3\text{CN}$  (left) and  $\text{DMF-d}_7$  (right) of cyclic azobenzene **1** before (top) and after *ex-situ* illumination (365 nm, 60 min; bottom).

### 3.2.2. Diiodo cyclic azobenzene **5**

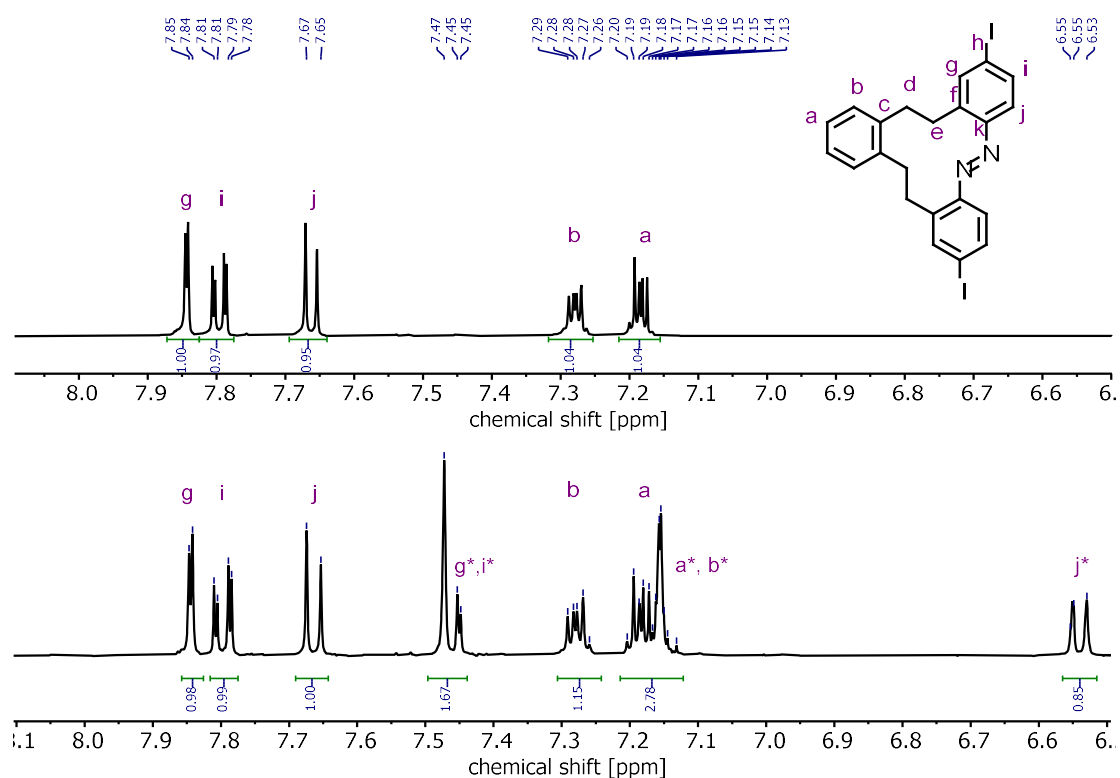


**Figure S28.** Partial  $^1\text{H}$  NMR spectra (500 MHz,  $\text{CD}_2\text{Cl}_2$ , 298 K) of the aromatic region of **5** before (top) and after (bottom) *ex-situ* irradiation at 365 nm for 60 min. Integration of the signals H-g and H-g\* gave a ratio of 45% Z-**5** in the sample.

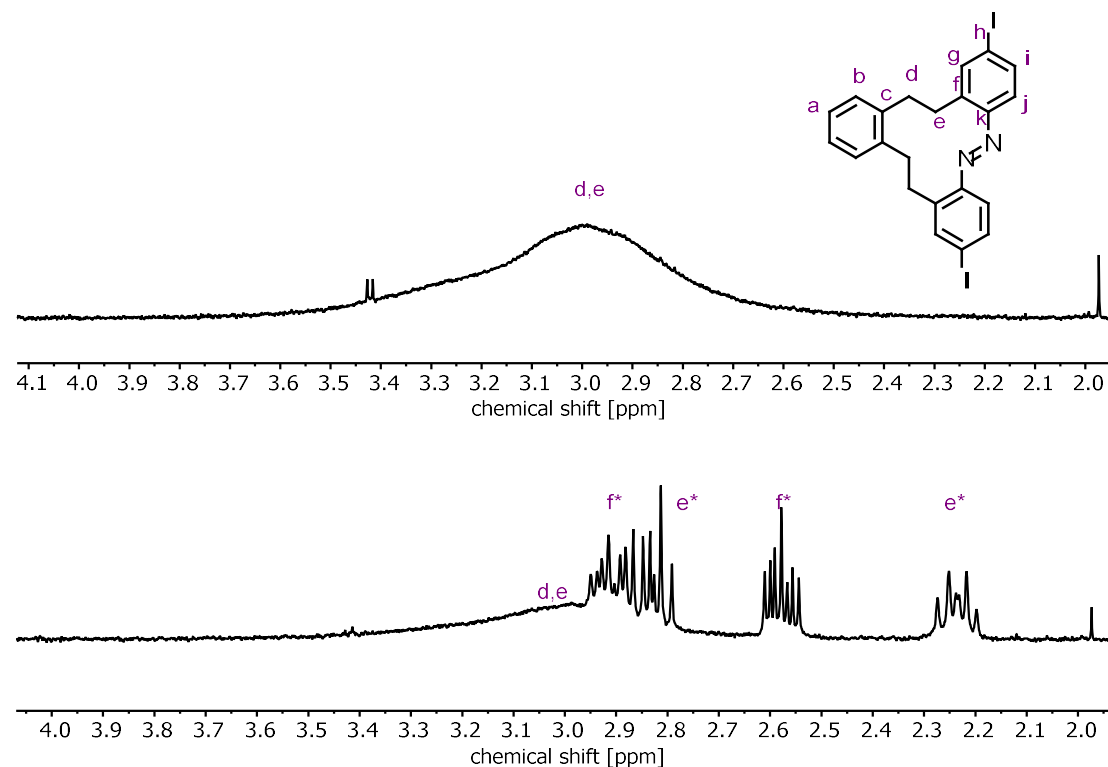


**Figure S29.** Partial  $^1\text{H}$  NMR spectra (500 MHz,  $\text{CD}_2\text{Cl}_2$ , 298 K) of the aliphatic region of **5** before (top) and after (bottom) *ex-situ* irradiation at 365 nm for 60 minutes. The previously broad signals for H<sub>d</sub> and H<sub>e</sub> in E-**5** appear as four distinct, sharp diastereotopic signals for Z-**5**.

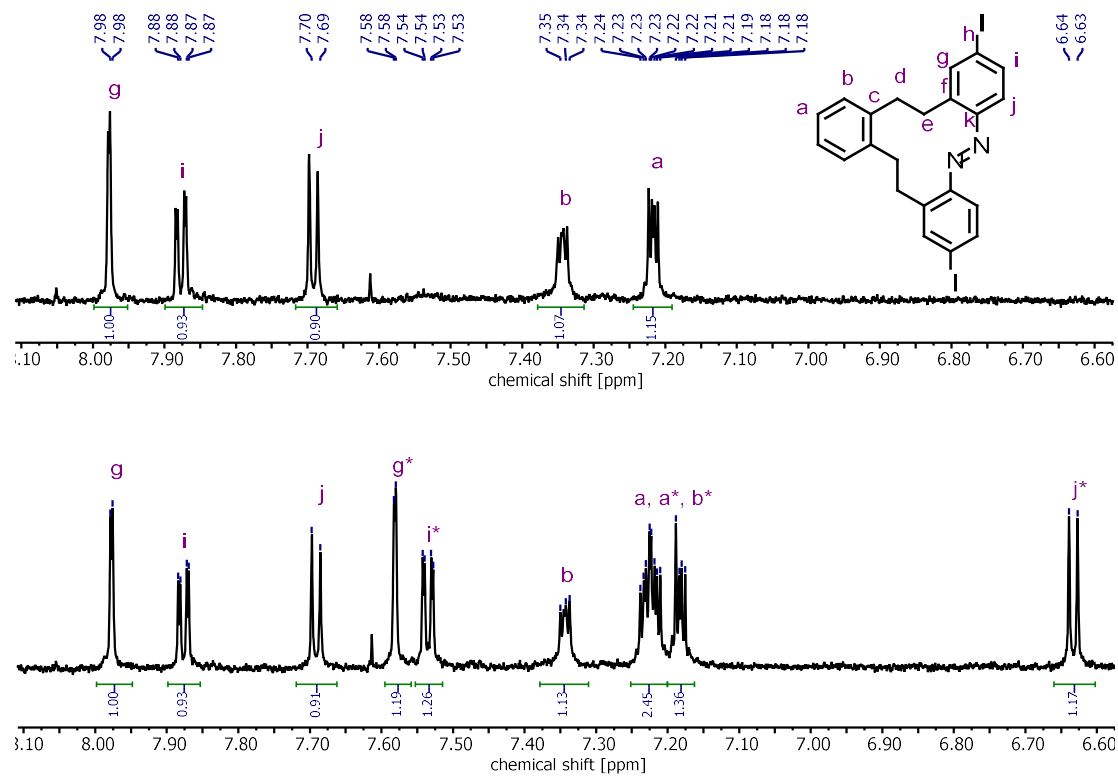


**Figure S30.** Partial  $^1\text{H}$  NMR spectra (700 MHz,  $\text{CD}_3\text{CN}$ , 298 K) of the aromatic region of **5** before (top) and after (bottom) *ex-situ* irradiation at 365 nm for 45 min. Integration of the signals H-g and H-g\* gave a ratio of 54% Z-**5** in the sample.

### 3.3. Determination of photostationary states (PSS) by HPLC and UV-vis spectroscopy

#### Method

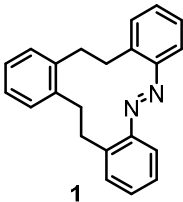
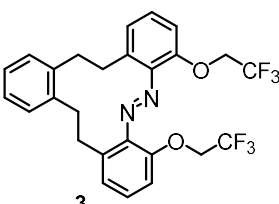
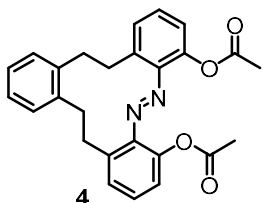
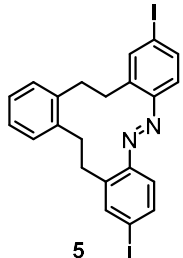
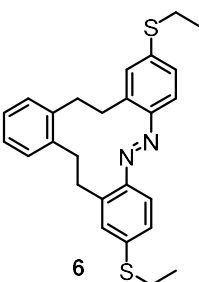
**Step 1 – determination of the optimal excitation wavelength.** To determine the optimal excitation wavelength  $\lambda_{\text{ex}}$ , the sample was irradiated for 5 minutes using different wavelengths and UV-vis spectra were recorded using a flash-lamp spectrometer. The excitation wavelength that resulted in the largest change in the UV-vis spectrum was used for further experiments.

**Step 2 – determination of isosbestic points.** The sample was irradiated using the optimal excitation wavelength  $\lambda_{\text{ex}}$  in one of the illumination setups described in Section 3.1 and UV-vis spectra were recorded in regular time intervals. The resulting spectra were stacked to identify the isosbestic point(s).

**Step 3 – HPLC run.** The samples were irradiated inside an amberised vial using the setup shown in **Figure S22** until the PSS was reached and injected into the HPLC with the lights in the room turned off. Since a reverse phase column (C18) was used, the more polar *Z*-form is expected to be eluting first and the less polar *E*-form after that. The chromatogram was plotted using one of the isosbestic points as the detector wavelength since the extinction coefficients of *E* and *Z*-isomers are identical at those points. Area-integration of the chromatogram gives PSS<sup>HPLC</sup> as determined by HPLC.<sup>5</sup>

**Step 4 – Fit of PSS from UV-vis spectra.** Due to the long half-lives of the compounds, UV-vis spectra of pure *E* and pure *Z*-isomers could be obtained from the HPLC runs using its internal UV-vis spectrometer. The absorbance of the *E*-isomer was scaled to be identical to the spectrum of a non-irradiated sample while the spectrum of the *Z*-isomer was scaled to intersect at the isosbestic point used in step 3. A UV-vis spectrum of the PSS obtained from the same sample (= exactly the same concentration) at the plate reader was fitted with a linear combination of the spectra of the *E* and *Z*-isomers to give the PSS<sup>Fit</sup>.<sup>5</sup>

**Table S3.** Overview over the results of the determination of the photo stationary states for **1**, **3**, **4**, **5**, and **6**. The derivatives **2** and **7** showed almost no change upon irradiation and were therefore not investigated further.

Compound	Isosbestic point	PSS <sup>HPLC</sup> (% Z) (CH <sub>3</sub> CN)	PSS <sup>Fit</sup> (% Z) (CH <sub>3</sub> CN / CH <sub>3</sub> OH 1:1 (v/v))	PSS <sup>NMR</sup> (% Z)
 <b>1</b>	276 nm	53%	51%	55% (CD <sub>3</sub> CN) 59% (DMF-d <sub>7</sub> ) 51% (CD <sub>2</sub> Cl <sub>2</sub> )
 <b>3</b>	296 nm	14%	14%	
 <b>4</b>	244 nm	34%	47%	
 <b>5</b>	287 nm	61% (Chromatogram not clean)	65%	54% (CD <sub>3</sub> CN) 45% (CD <sub>2</sub> Cl <sub>2</sub> )
 <b>6</b>	347 nm	38%	45%	

### 3.3.1. Cyclic azobenzene 1

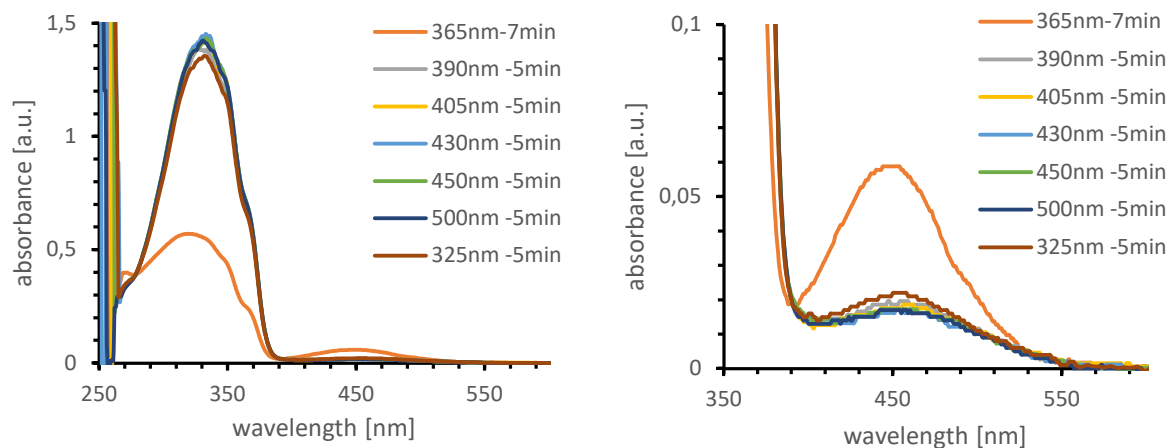


**Figure S31.** UV-vis spectra of **1** (DMF, 1 mM) after irradiation with different wavelengths (325, 365, 390, 405, 430, 450, and 500 nm, respectively) to determine the optimal excitation wavelength for photoswitching of **1**.

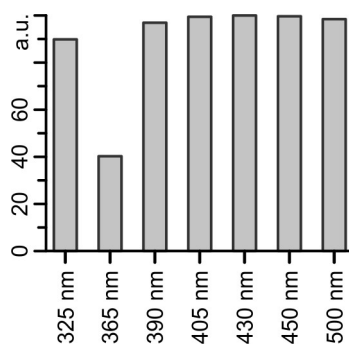


**Figure S32.** Absorptions of **1** at 330 nm (1 mM, DMF) after irradiations with light of different wavelengths demonstrating *E-1* to be the favoured isomer under any wavelength except 365 nm.

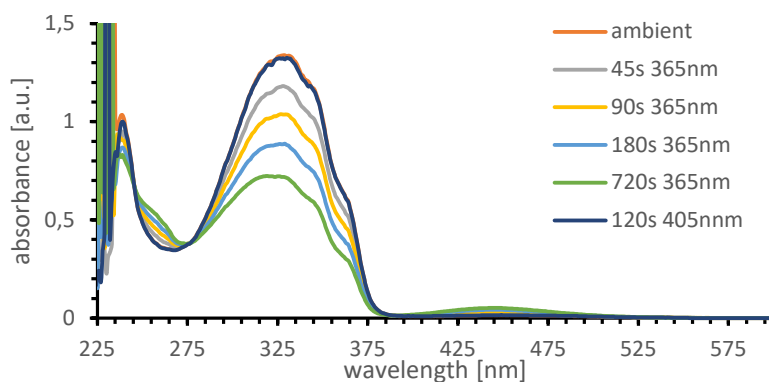


**Figure S33.** Irradiation of **1** (MeCN/MeOH 1:1 (v/v), 1 mM) with 365 nm light for different time intervals (45, 90, 120, 180, and 720 s, respectively) showing isosbestic points at 246 nm and 276 nm.

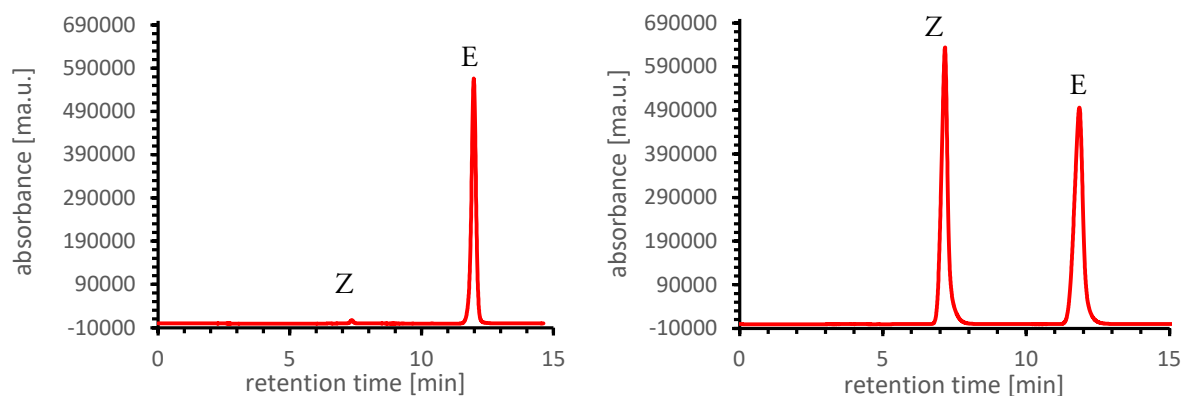


**Figure S34.** HPLC chromatogram (MeCN/MeOH 1:1 (v/v)) at 276.5 nm of **1** after standing on a sunny windowsill for 2 h showing 1% Z-1 (left) and of the PSS<sup>365</sup> of **1** (irradiated for 30 min @365nm, 1 mM in MeCN) showing 51% Z-1 (right).

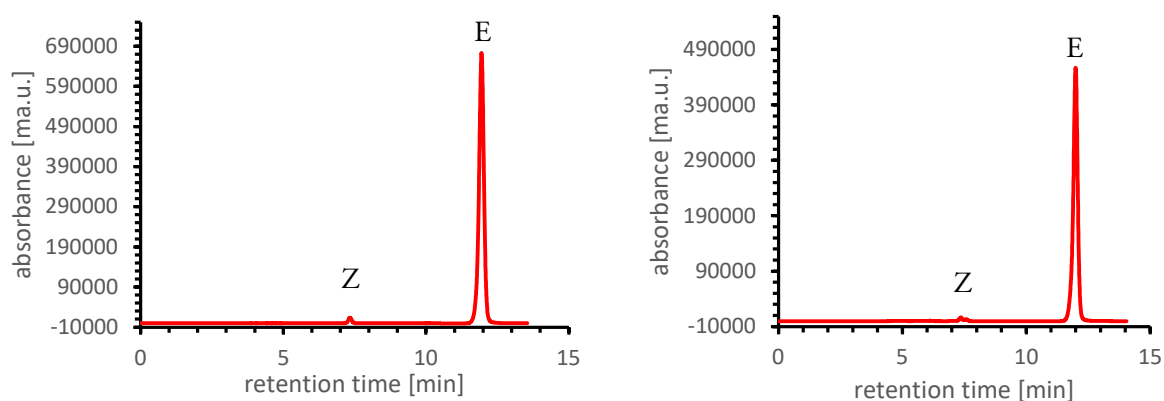


**Figure S35.** HPLC chromatogram (MeCN/MeOH 1:1 (v/v)) at 276.5 nm of the PSS<sup>405</sup> of **1** (irradiated for 30 min @405nm, 1 mM in MeCN) showing 1% Z-1(left) and of the PSS<sup>450</sup> of **1** (irradiated for 30 min @450nm, 1 mM, MeCN) showing 1% Z-1(right).

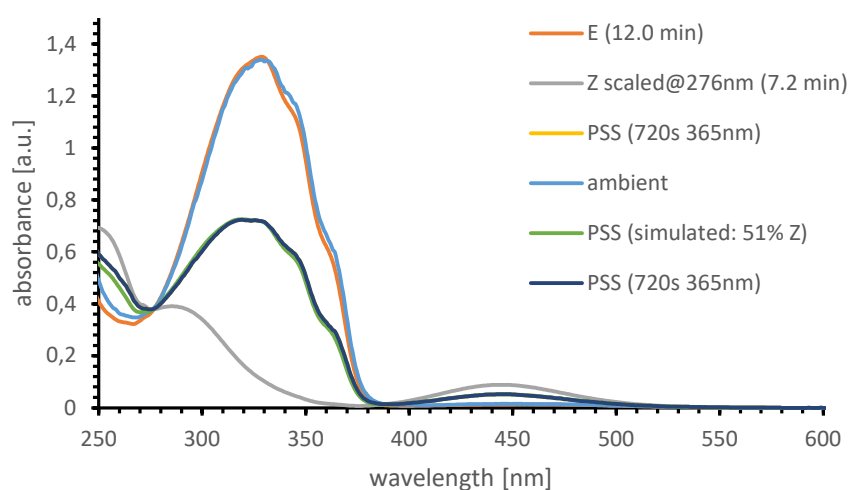


**Figure S36.** UV-vis spectra (CH<sub>3</sub>CN/CH<sub>3</sub>OH 1:1 (v/v)) of **E-1** (blue, normalized) and **Z-1** (green, normalized) as obtained after HPLC separation, **1** subjected to ambient light (orange, 1 mM), PSS of **1** after 12 min irradiation with 365 nm light (yellow, 1 mM), and the simulated spectrum of the PSS<sup>fit</sup> of **1** showing 51% Z-1 (grey).

### 3.3.2. Dimethoxy cyclic azobenzene **2**

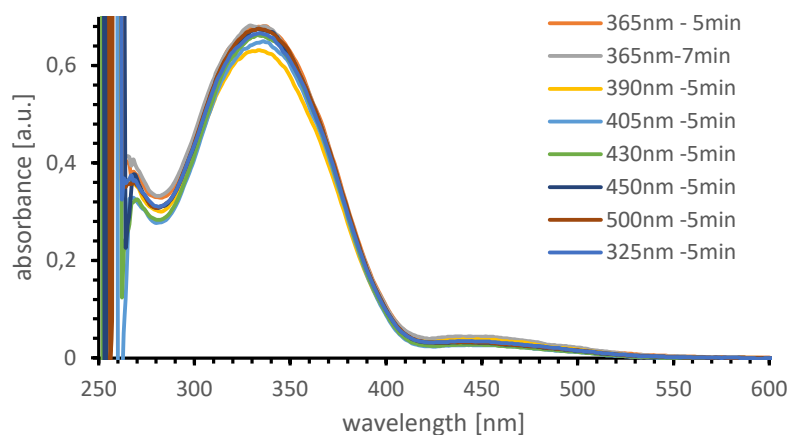


**Figure S37.** UV-vis spectra of **2** (DMF, 1 mM) after irradiation with different wavelengths (325, 365, 390, 405, 430, 450, and 500 nm, respectively) to determine the optimal excitation wavelength for photoswitching of **2**.

Compound **2** only showed slight changes in its absorption spectrum after irradiation at 390 nm and 405 nm. This shows that the excitation wavelength had been redshifted, but the difference before and after irradiation was rather small. This suggests a very low amount of *Z*-**2** being present. Due to this bad switching behaviour the photophysical properties of **2** were not investigated further.



### 3.3.3. Bis(trifluoroethoxy) cyclic azobenzene 3

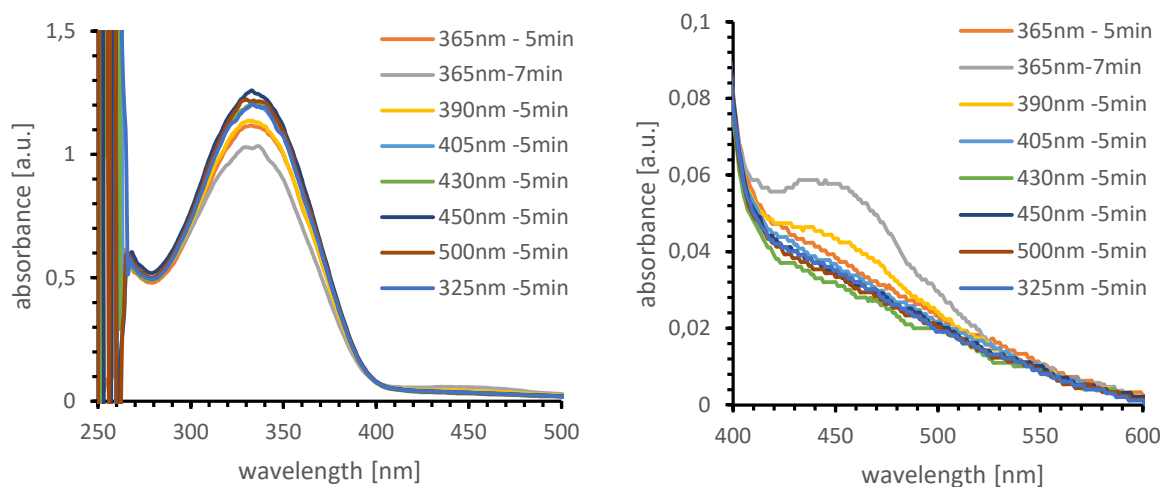


**Figure S38.** UV-vis spectra of **3** (DMF, 1 mM) after irradiation with different wavelengths (325, 365, 390, 405, 430, 450, and 500 nm, respectively) to determine the optimal excitation wavelength for photoswitching of **3**.

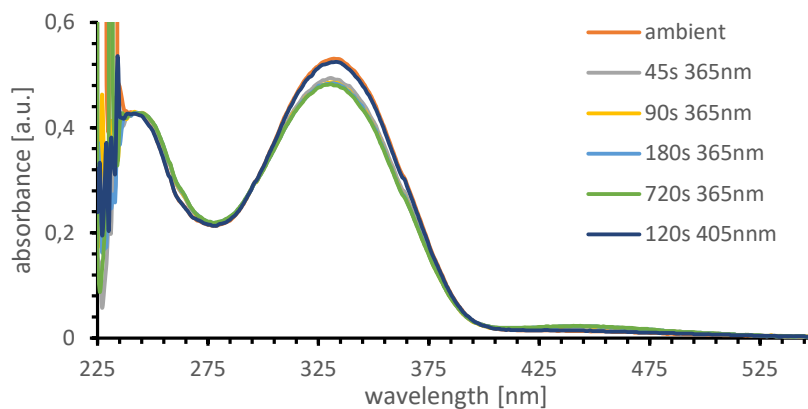


**Figure S39.** Irradiation of **3** (MeCN/MeOH 1:1 (v/v), 1 mM) with 365 nm light for different time intervals (45, 90, 120, 180, and 720 s, respectively) showing an isosbestic point at 296 nm.

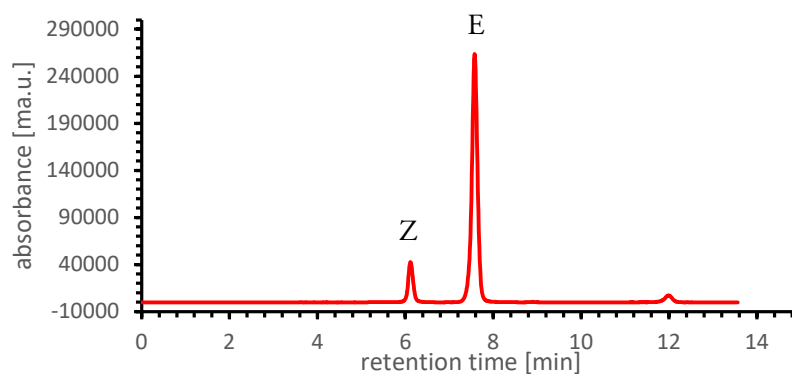


**Figure S40.** HPLC chromatogram (MeCN/MeOH 1:1 (v/v)) at 269.3 nm of the PSS<sup>365</sup> of **3** (irradiated for 30 min @365nm, 1 mM in MeCN) showing 14% Z-**3**.

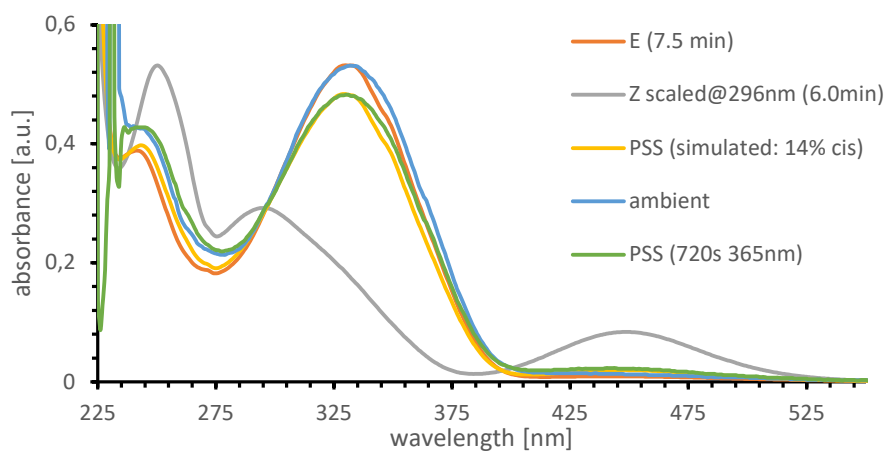


**Figure S41.** UV-vis spectra ( $\text{CH}_3\text{CN}/\text{CH}_3\text{OH}$  1:1 (v/v)) of **E-3** (orange, normalized) and **Z-3** (yellow, normalized) as obtained after HPLC separation, **3** subjected to ambient light (blue, 1 mM), PSS of **3** after 12 min irradiation with 365 nm light (green, 1 mM), and the simulated spectrum of the PSS<sup>fit</sup> of **3** showing 14% **Z-3** (grey).

### 3.3.4. Diaceto cyclic azobenzene 4

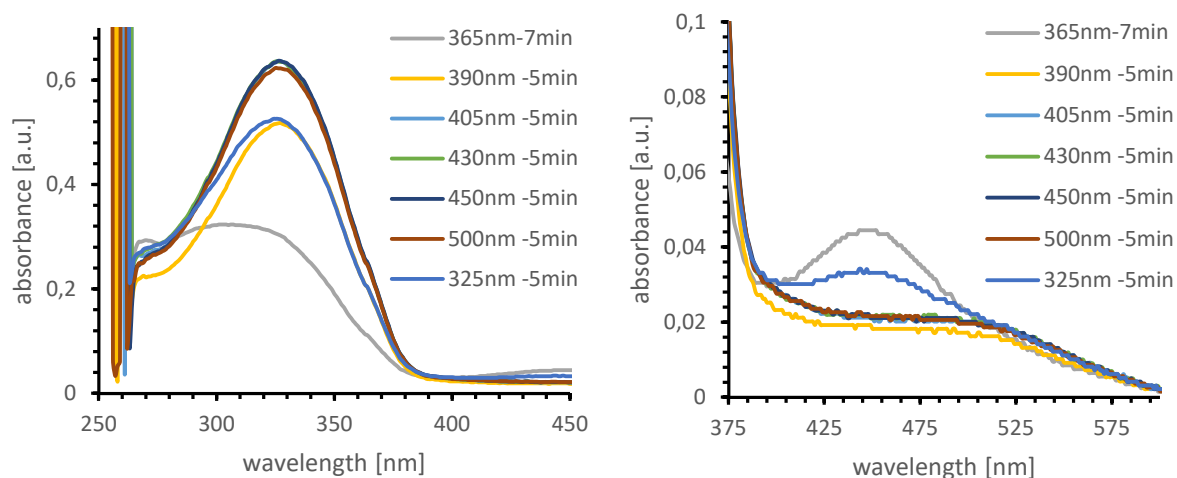


**Figure S42.** UV-vis spectra of **4** (DMF, 1 mM) after irradiation with different wavelengths (325, 365, 390, 405, 430, 450, and 500 nm, respectively) to determine the optimal excitation wavelength for photoswitching of **4**.

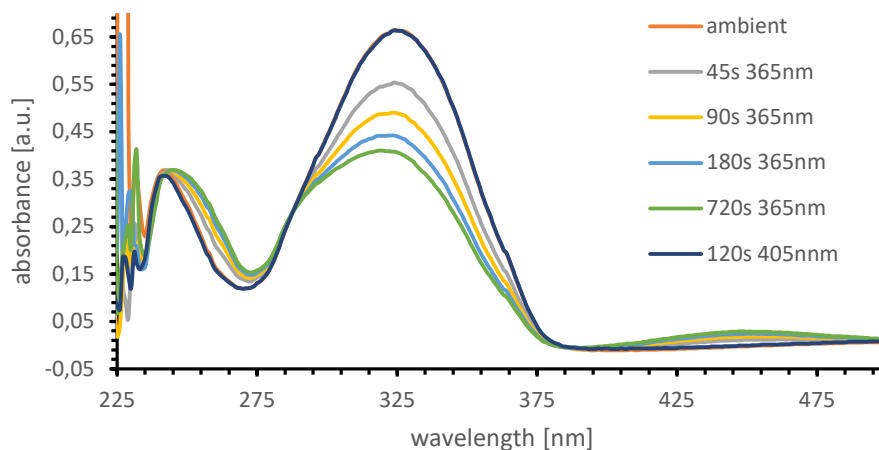


**Figure S43.** Irradiation of **4** (MeCN/MeOH 1:1 (v/v), 1 mM) with 365 nm light for different time intervals (45, 90, 120, 180, and 720 s, respectively) showing isosbestic points at 244 nm and 288 nm.

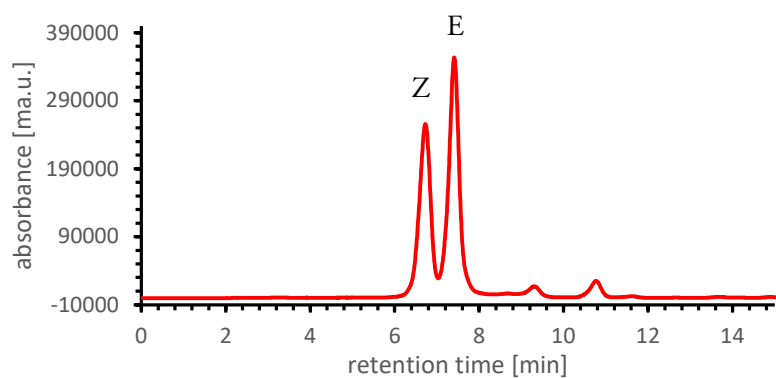


**Figure S44.** HPLC chromatogram (MeCN/MeOH 1:1 (v/v)) at 244.4 nm of the PSS<sup>365</sup> of **4** (irradiated for 30 min @365nm, 1 mM in MeCN) showing 34% Z-**4**.

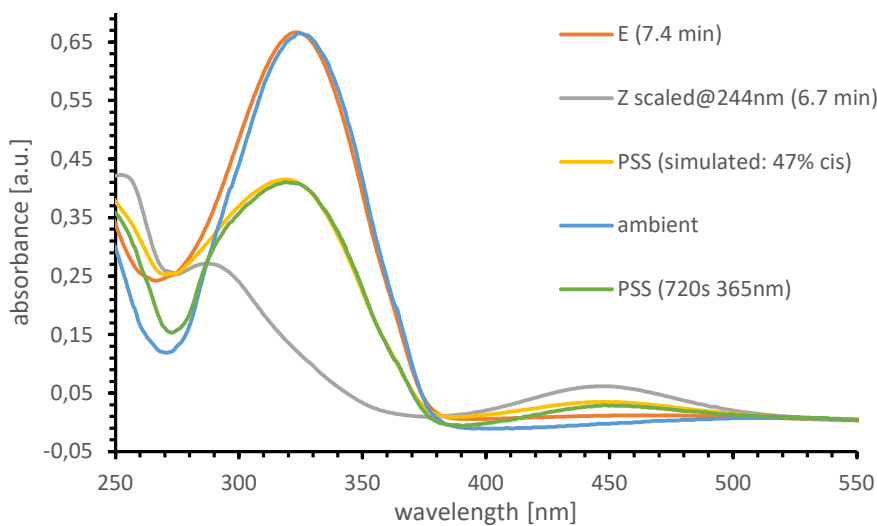


**Figure S45.** UV-vis spectra (CH<sub>3</sub>CN/CH<sub>3</sub>OH 1:1 (v/v)) of **E-4** (orange, normalized) and **Z-4** (grey, normalized) as obtained after HPLC separation, **4** subjected to ambient light (blue, 1 mM), PSS of **4** after 12 min irradiation with 365 nm light (green, 1 mM), and the simulated spectrum of the PSS<sup>fit</sup> of **4** showing 47% Z-**4** (yellow).

### 3.3.5. Diiodo cyclic azobenzene 5

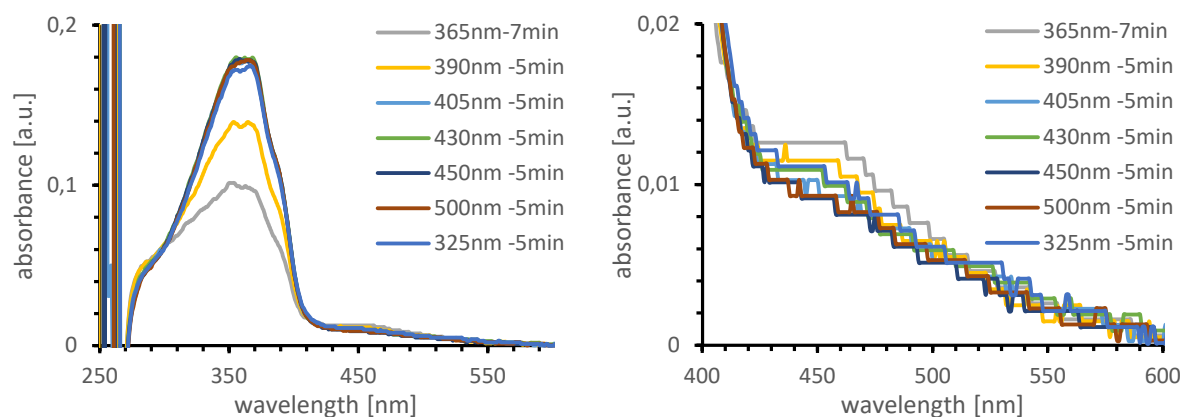


**Figure S46.** UV-vis spectra of **5** (DMF, 1 mM) after irradiation with different wavelengths (325, 365, 390, 405, 430, 450, and 500 nm, respectively) to determine the optimal excitation wavelength for photoswitching of **5**.

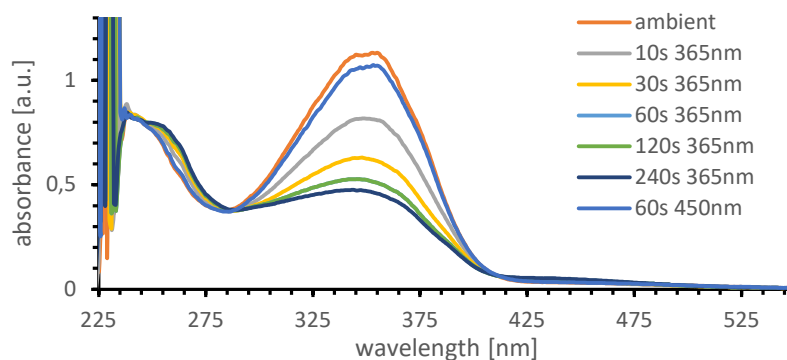


**Figure S47.** Irradiation of **5** (MeCN/MeOH 1:1 (v/v), 1 mM) with 365 nm light for different time intervals (45, 90, 120, 180, and 720 s, respectively) showing isosbestic points at 287 nm and 412 nm.

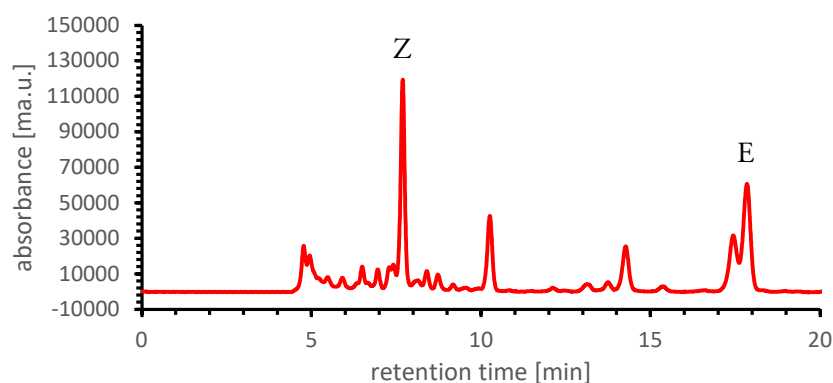


**Figure S48.** HPLC chromatogram (MeCN/MeOH 1:1 (v/v)) at 287.6 nm of the PSS<sup>365</sup> of **5** (irradiated for 30 min @365nm, 1 mM in MeCN) showing 61% Z-**5**.

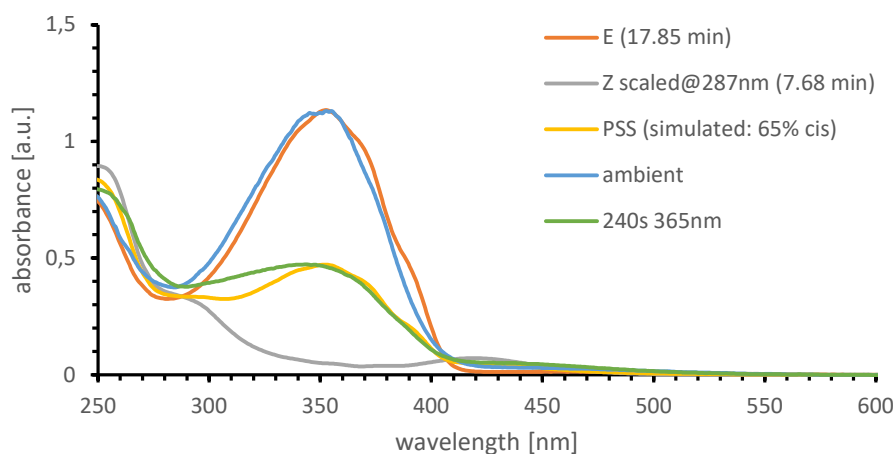


**Figure S49.** UV-vis spectra ( $\text{CH}_3\text{CN}/\text{CH}_3\text{OH}$  1:1 (v/v)) of **E-5** (orange, normalized) and **Z-5** (grey, normalized) as obtained after HPLC separation, **5** subjected to ambient light (blue, 1 mM), PSS of **5** after 4 min irradiation with 365 nm light (green, 1 mM), and the simulated spectrum of the PSS<sup>fit</sup> of **5** showing 65% **Z-5** (yellow).

The HPLC chromatogram showed multiple other peaks that could not be removed by repeated column chromatography and the resulting PSS<sup>HPLC</sup> at 365 nm might therefore be inaccurate. Small contaminations by a strongly absorbing contamination might also affect PSS<sup>fit</sup> resulting from the fitted UV-vis spectrum quite significantly. These contaminations were not visible in the <sup>1</sup>H NMR spectra. Therefore, an irradiated sample was investigated using <sup>1</sup>H NMR spectroscopy (see *ex-situ* irradiation in Section 3.2). Integration of the signals gave a ratio of 45% **Z-5** in the sample.

### 3.3.6. Thioether substituted cyclic azobenzene 6

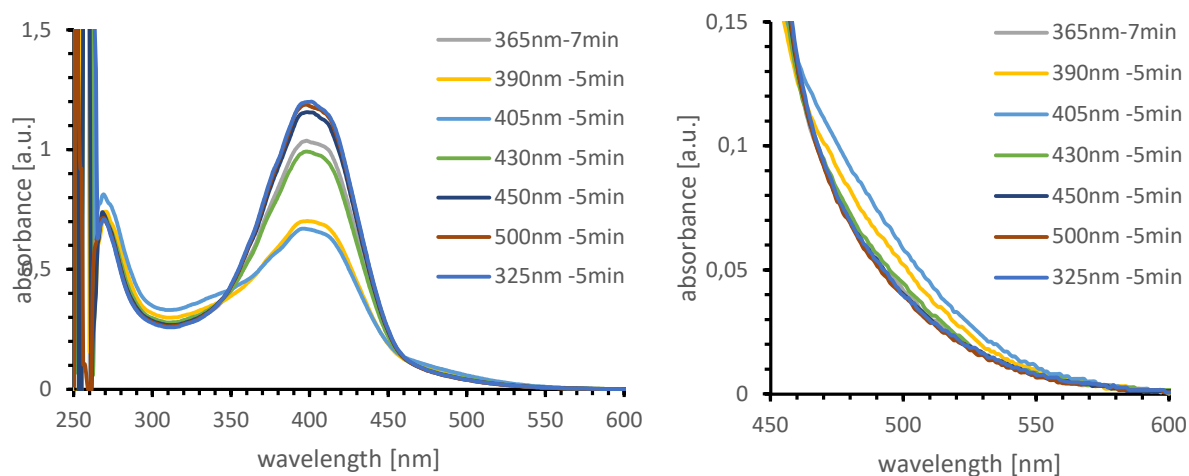


**Figure S50.** UV-vis spectra of **6** (DMF, 1 mM) after irradiation with different wavelengths (325, 365, 390, 405, 430, 450, and 500 nm, respectively) to determine the optimal excitation wavelength for photoswitching of **6**.

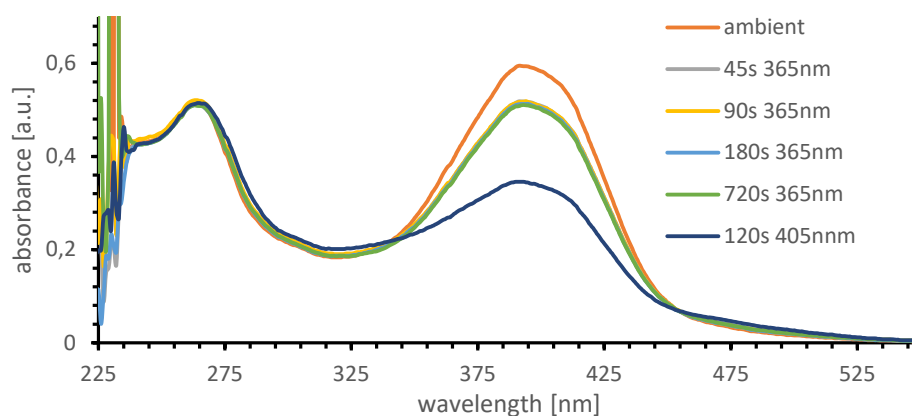


**Figure S51.** Irradiation of **6** (MeCN/MeOH 1:1 (v/v), 1 mM) with 365 nm light for different time intervals (45, 90, 120, 180, and 720 s, respectively) showing isosbestic points at 347 nm and 455 nm.

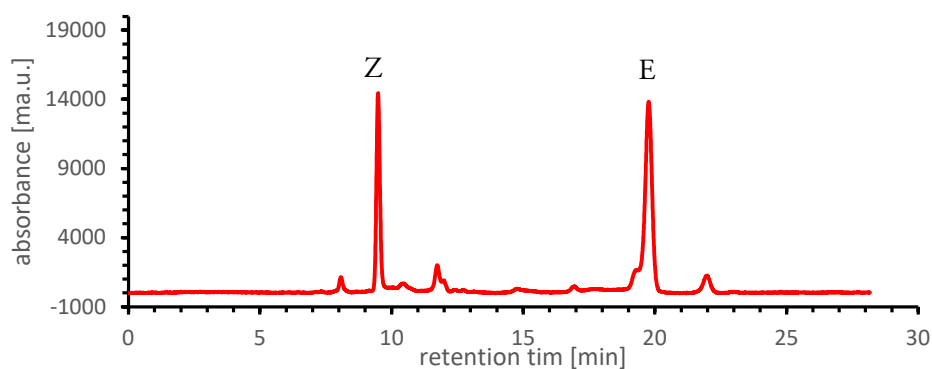


**Figure S52.** HPLC chromatogram (MeCN/MeOH 1:1 (v/v)) at 454.7 nm of the PSS<sup>405</sup> of **6** (irradiated for 30 min @405nm, 1 mM in MeCN) showing 38% **Z-6**.

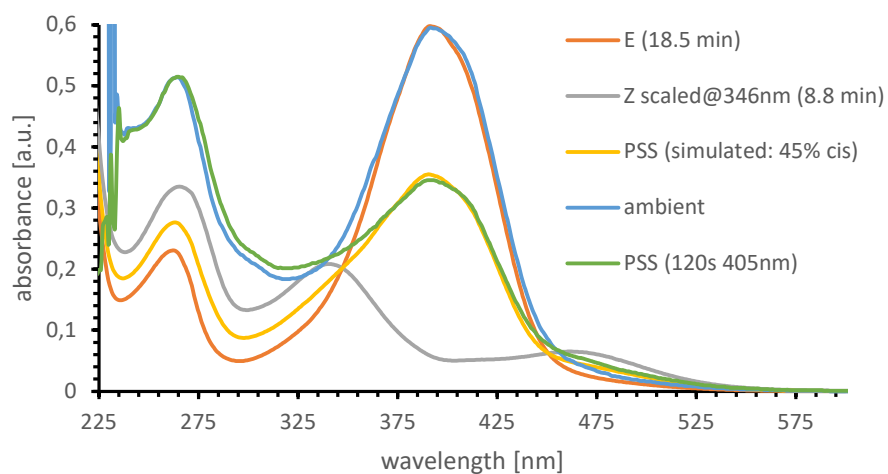


**Figure S53.** UV-vis spectra ( $\text{CH}_3\text{CN}/\text{CH}_3\text{OH}$  1:1 (v/v)) of **E-6** (orange, normalized) and **Z-6** (grey, normalized) as obtained after HPLC separation, **6** subjected to ambient light (blue, 1 mM), PSS of **6** after 2 min irradiation with 405 nm light (green, 1 mM), and the simulated spectrum of the PSS<sup>fit</sup> of **4** showing 45% **Z-6** (yellow).



### 3.3.7. bis(4-methoxyphenyl)phenylamine substituted cyclic azobenzene 7

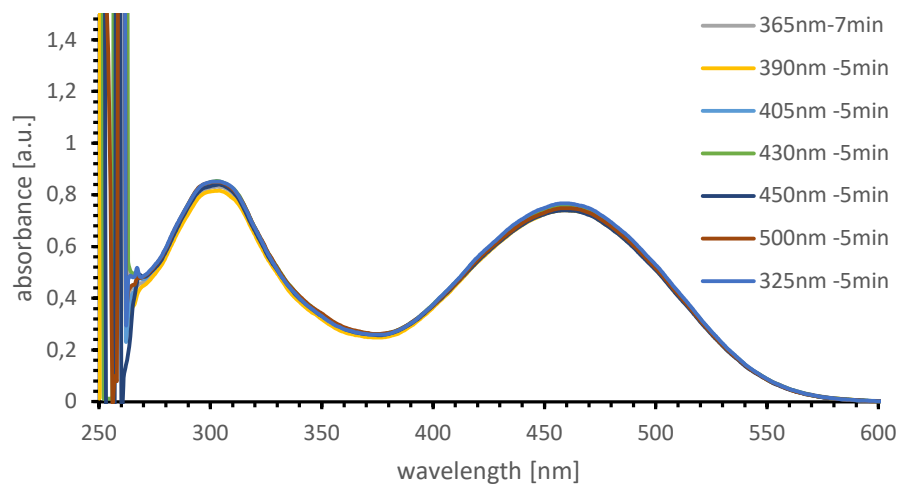


**Figure S54.** UV-vis spectra of **7** (DMF, 1 mM) after irradiation with different wavelengths (325, 365, 390, 405, 430, 450, and 500 nm, respectively) to determine the optimal excitation wavelength for photoswitching of **7**.

Compound **7** showed basically no changes in its absorption spectrum after irradiation at any wavelength. This suggests that either no *Z-7* is being formed or thermal relaxation is extremely fast. Due to this bad switching behaviour, the photophysical properties of **7** were not investigated further.

### 3.4. Determination of thermal half-lives $\tau_{1/2}$ by UV-vis and $^1\text{H}$ NMR spectroscopy

#### General procedure for the NMR method

An NMR sample was prepared in  $\text{CD}_3\text{CN}$  and irradiated for 60 minutes in a brown glass vial that had been covered in aluminium foil using the 365 nm LED. In a dark room, the sample was transferred to an amberised NMR tube. The sample was placed inside of the spectrometer that had been heated to 45 °C and  $^1\text{H}$  NMR spectra were recorded every 30 minutes for 72 h.

A well visible proton signal was chosen, and the corresponding signals in  $Z$ - and  $E$ -state integrated. The integrals were used to calculate the percentage of the excited  $Z$  isomer which was normalized and plotted against the time  $t$  and fitted using first order kinetics (**Equation S1**) to give rate constants  $k$  and the half-lives  $\tau_{1/2} = \ln(2) \cdot k^{-1}$  (**Table S4**).

$$\%_{0_t}^{Z,\text{normalized}} = \frac{\%_t^Z - \%_{\infty}^Z}{\%_0^Z - \%_{\infty}^Z} = e^{-kt} \quad \text{using: } \%_x^Z = \frac{I_x^Z}{I_x^Z + I_x^E} \quad (\text{S1})$$

**Table S4.** Rate constants  $k$ , mean lifetimes  $\tau = k^{-1}$ , and half-lives  $\tau_{1/2}$  obtained by thermal relaxation experiments of **1** using  $^1\text{H}$  NMR (45 °C,  $\text{CD}_3\text{CN}$ , 50 mM).

	<b>1</b>
$\tau_{1/2}$ [h]	35.6
$\tau$ [h]	51.3
$k$ [ $\text{h}^{-1}$ ]	0.0195

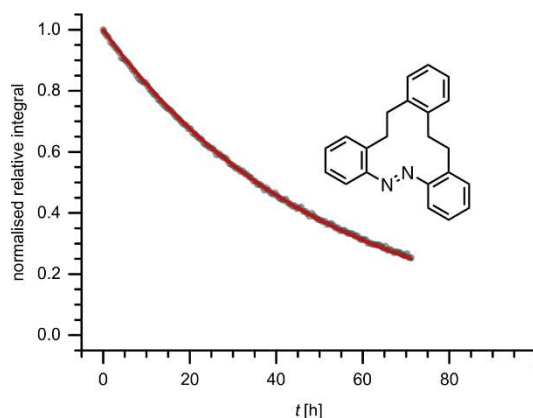


**Figure S55.** Thermal relaxation of **1** in  $\text{CD}_3\text{CN}$  (50  $\text{mmol L}^{-1}$ ) at 45 °C after irradiation at 365 nm for 60 minutes.

### General procedure for the UV-vis method

First, a reference spectrum was taken of a 96-well plate containing multiple samples of each compound in DMF (1 mmol L<sup>-1</sup>). The plate was then irradiated at 365nm for 40 minutes and placed in the plate reader that had been preheated to 45 °C. A UV-vis spectrum was measured every two hours.

One wavelength that showed significant changes in intensity was chosen for each compound. Using the spectra taken before irradiation this absorbance was normalized and plotted against the time  $t$  and fitted using first order kinetics (**Equation S2**) to give rate constants  $k$  and the half-lives  $\tau_{1/2} = \ln(2) \cdot k^{-1}$  (**Table S5**).

$$A^{\text{normalized}} = \frac{A_t - A_\infty}{A_0 - A_\infty} = e^{-kt} \quad (\text{S2})$$

**Table S5.** Rate constants  $k$ , mean lifetimes  $\tau = k^{-1}$ , and half-lives  $\tau_{1/2}$  obtained by thermal relaxation experiments of **1**, **3**, **4**, **5**, and **6** (45 °C, DMF, 1 mM) using UV-Vis. Relaxation of **1** was also investigated at ambient temperature (DMF, 1 mM). Multiple replicates were performed for each photoswitch as indicated.  $\lambda_{\text{fit}}$  indicates the wavelength at which the absorption was followed.

	<b>1</b>		<b>3</b>	<b>4</b>	<b>5</b>	<b>6</b>
$\lambda_{\text{fit}}$ [nm]	330	330	330	330	360	400
replicates	4	4	6	6	4	5
$\tau_{1/2}$ [h]	30.6 (45 °C)	379 (ambient $T$ )	8.2	7.1	19	1.23
$\tau$ [h]	44.2 (45 °C)	547 (ambient $T$ )	11.8	10.2	27	1.77
$k$ [h <sup>-1</sup> ]	0.0226 (45 °C)	0.0018 (ambient $T$ )	0.0847	0.0980	0.0370	0.5650

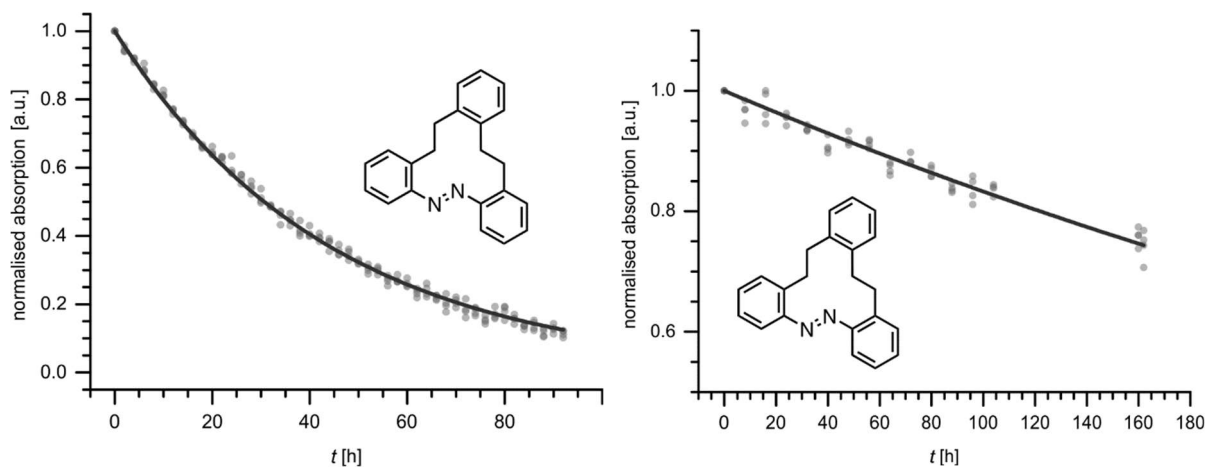


**Figure S56.** Thermal relaxation of **1** in DMF ( $1 \text{ mmol L}^{-1}$ ) at 45 °C (left) and ambient  $T$  (right) after irradiation at 365 nm for 40 minutes. Both graphs are a combination of four replicates.

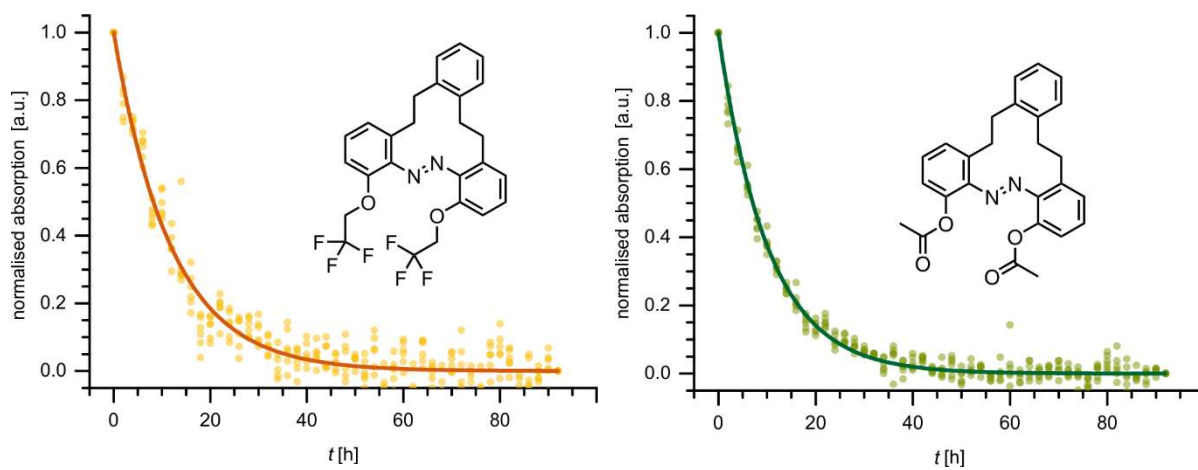


**Figure S57.** Thermal relaxation of **3** (left) and **4** (right) in DMF ( $1 \text{ mmol L}^{-1}$ ) at 45 °C after irradiation at 365 nm for 40 minutes. Both graphs are a combination of six replicates.

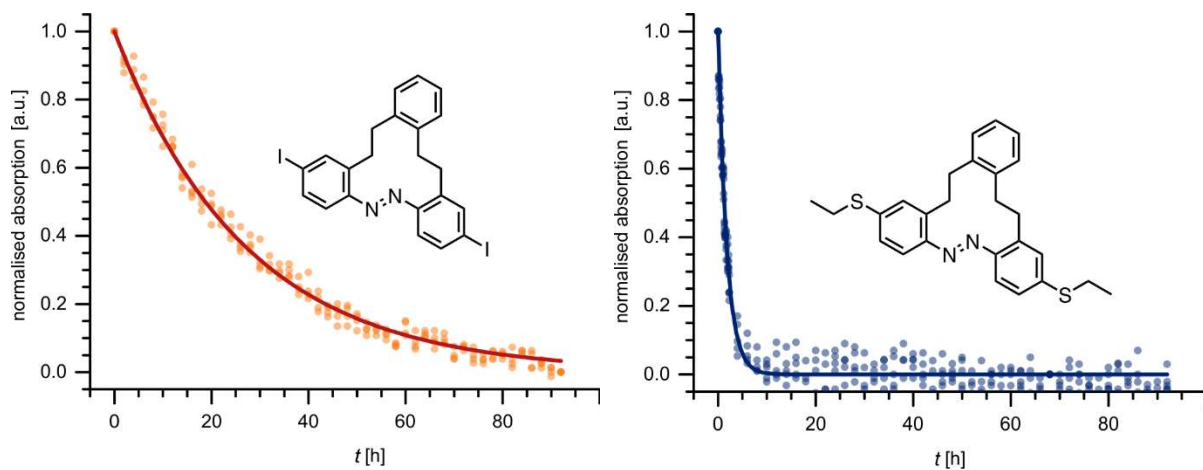


**Figure S58.** Thermal relaxation of **5** (left) and **6** (right) in DMF ( $1 \text{ mmol L}^{-1}$ ) at  $45 \text{ }^\circ\text{C}$  after irradiation at  $365 \text{ nm}$  for 40 minutes. The left graph contains 4 replicates, and the right graph contains 5 replicates.

### 3.5. Reversibility of photoisomerization

Solutions of **1**, **4**, and **5** in DMF ( $1 \text{ mmol L}^{-1}$ ) were prepared in a 96-well plate and a reference UV-vis spectrum was measured. The sample was then irradiated for 15 minutes alternating between 365nm and white light. UV-vis spectra were recorded in between the irradiation steps and absorbances at 330 nm plotted against the number of cycles (**Figure S59**, **Figure S60**, and **Figure S61**). Compounds **1** and **4** showed no degradation over 20 cycles while slight degradation could be observed for **5**.

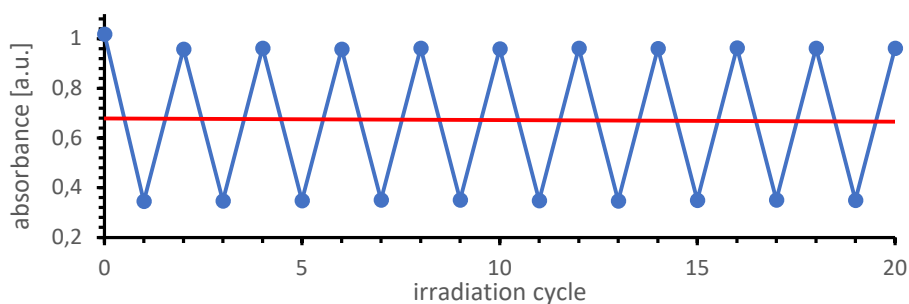


**Figure S59.** Absorbance at 330 nm with alternating irradiations at 365 nm and with white light demonstrating reversible photoisomerization cycles of compound **1** (1 mM, DMF).

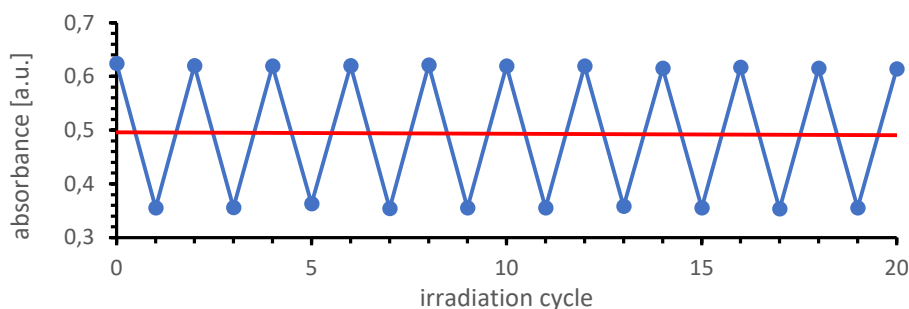


**Figure S60.** Absorbance at 330 nm with alternating irradiations at 365 nm and with white light demonstrating reversible photoisomerization cycles of compound **4** (1 mM, DMF).

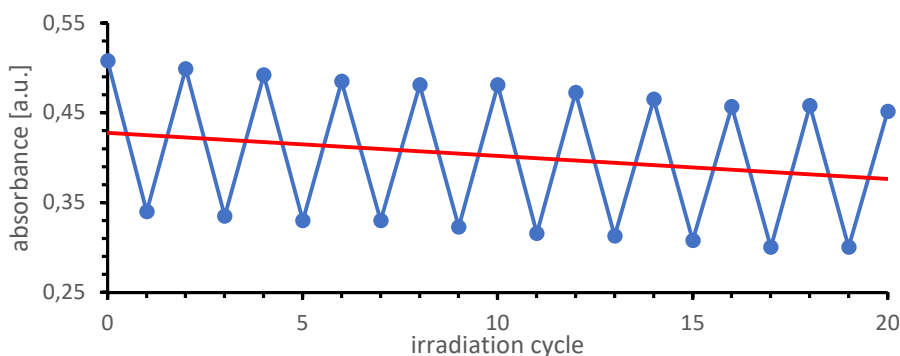


**Figure S61.** Absorbance at 330 nm with alternating irradiations at 365 nm and with white light showing slight photodegradation of compound **5** (1 mM, DMF) during the irradiation cycles.

#### 4. Quantum chemical calculations

Geometries were optimized and energies calculated on DFT level using the range separated wb97x-v hybrid functional<sup>6</sup> on a def2-QZVP<sup>7</sup> level of theory using Orca 5.0.3.<sup>8,9</sup> The total energy was calculated using **Equation S2** with the gas phase energy at 0 K calculated by DFT ( $E^{0K}$ ), the thermodynamic contribution  $dG^T$  and the solvation free energy corresponding to the change from gas phase to the solvent  $dG^{solv}$ .

$$dG^{total} = E^{0K} + dG^T + dG^{solv} \quad (S2)$$

The thermodynamic contribution  $dG^T$  was calculated using a modified rigid-rotor harmonic-oscillator approach (mRRHO<sup>10</sup>) with frequencies calculated using the r2scan-3c composite method<sup>11</sup> and  $dG^{solv}$  was calculated using the conductor like screening model for realistic solvation (COSMO-RS).<sup>12,13</sup> The results of these calculations are presented in **Table S6**.

The resulting structures are shown in Figure S62 and additionally provided as separate xyz files.

**Table S6.** Results of quantum chemical calculations.

	$E^{0K}$	$dG^T$	$dG^{solv}$ (DCM)	$dG^{total}$	$ddG^{total}$ [kJ mol <sup>-1</sup> ]
Z-1	-959.97069	0.31869	-0.02712	-959.67912	0
E-1	-959.9934	0.31846	-0.02533	-959.70027	55.6

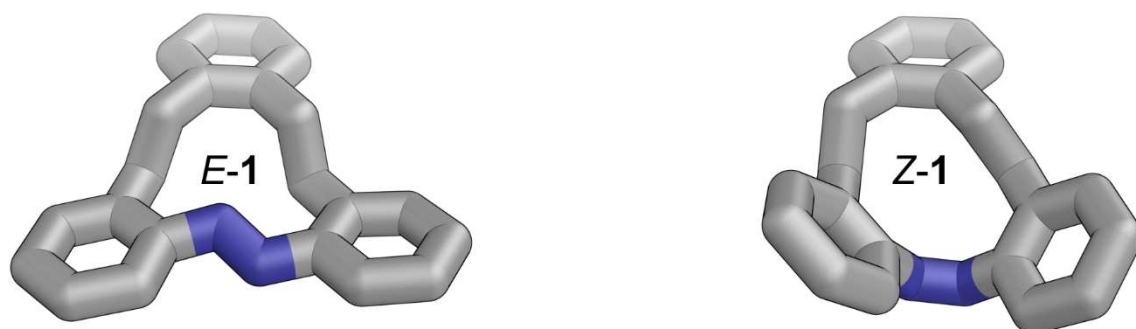


**Figure S62.** Optimized structures of E-1 and Z-1.

## 5. Crystal structure

Suitable clear orange plank-like single crystals of **E-1** were grown upon slow evaporation of its saturated solution in Dichloromethane at ca. 15 °C for about 4 weeks. The data collection was performed on a STOE Stadivari Eulerian 4-circle diffractometer using Cu-K $\alpha$  radiation ( $\lambda = 1.54186 \text{ \AA}$ ). The diffractometer was equipped with a low-temperature device (Cryostream 800er series, Oxford Cryosystems, 100(1) K). Intensities were measured by fine-slicing  $\omega$ -scans and corrected for background, polarization and Lorentz effects. An absorption correction by scaling of reflection intensities with a subsequent spherical absorption correction was performed with STOE LANA programme.<sup>14</sup>

The structure was solved by intrinsic phasing methods<sup>15</sup> and refined anisotropically by the least-squares procedure implemented in the SHELX programme system.<sup>16</sup> The hydrogen atoms were included isotropically using the riding model on the bound carbon atoms.

The correct assignment of the absolute configuration was done via the Flack parameter<sup>17</sup> (Flack(x) = -0.02(12)) and by using Bayesian statistics on Bijvoet differences giving the a P2(true) and P3(true) probability of 1.000, the probability of racemic twinning with  $0.5 \cdot 10^{-6}$ , and the probability of the assignment of the wrong absolute structure with  $0.2 \cdot 10^{-23}$ .<sup>18</sup>

CCDC number 2248689 contains the supplementary crystallographic data for this paper, which can be obtained free of charge from the Cambridge Crystallographic Data Centre via [http://www.ccdc.cam.ac.uk/data\\_request/cif](http://www.ccdc.cam.ac.uk/data_request/cif).

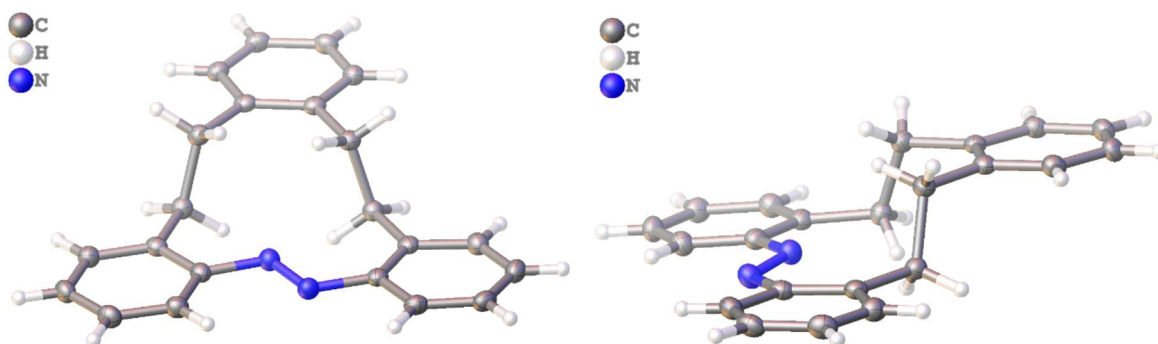


**Figure S63.** Asymmetric unit of cyclic azobenzene **1** as observed in the crystal structure, plotted from two different viewing angles. Hydrogen atoms omitted for clarity. Displacement ellipsoids are drawn at 50% probability.



**Table S7.** Crystal data and refinement parameters for cyclic azobenzene **1**.

Crystal Habitus	clear orange plank
Device Type	STOE STADIVARI
Empirical formula	C <sub>22</sub> H <sub>20</sub> N <sub>2</sub>
Moiety formula	C <sub>22</sub> H <sub>20</sub> N <sub>2</sub>
Formula weight	312.40
Temperature/K	100.15
Crystal system	orthorhombic
Space group	P2 <sub>1</sub> 2 <sub>1</sub> 2 <sub>1</sub>
a/Å	4.96650(10)
b/Å	11.8329(2)
c/Å	27.6027(5)
α/°	90
β/°	90
γ/°	90
Volume/Å <sup>3</sup>	1622.16(5)
Z	4
ρ <sub>calc</sub> /cm <sup>3</sup>	1.279
μ/mm <sup>-1</sup>	0.576
F(000)	664.0
Crystal size/mm <sup>3</sup>	0.32 × 0.207 × 0.14
Absorption correction	multi-scan
Tmin; Tmax	0.6362; 0.6934
Radiation	CuKα (λ = 1.54186)
2θ range for data collection/°	6.404 to 140.964°
Completeness to theta	1.000
Index ranges	-6 ≤ h ≤ 2, -13 ≤ k ≤ 14, -32 ≤ l ≤ 33
Reflections collected	65728
Independent reflections	3071 [R <sub>int</sub> = 0.0211, R <sub>sigma</sub> = 0.0056]
Data/restraints/parameters	3071/0/218
Goodness-of-fit on F <sup>2</sup>	1.050
Final R indexes [I >= 2σ (I)]	R <sub>1</sub> = 0.0249, wR <sub>2</sub> = 0.0641
Final R indexes [all data]	R <sub>1</sub> = 0.0251, wR <sub>2</sub> = 0.0643
Largest diff. peak/hole / e Å <sup>-3</sup>	0.18/-0.12
Flack parameter	-0.02(12)

## 6. References

- 1 M. S. Maier, K. Hüll, M. Reynders, B. S. Matsuura, P. Leippe, T. Ko, L. Schäffer and D. Trauner, *J. Am. Chem. Soc.*, 2019, **141**, 17295–17304.
- 2 A. Müller-deku and O. Thorn-seshold, *ChemRxiv*, 2022, **20**, 1–6.
- 3 C. Feldmeier, H. Bartling, E. Riedle and R. M. Gschwind, *J. Magn. Reson.*, 2013, **232**, 39–44.
- 4 S. Ghosh, C. Eschen, N. Eleya and A. Staubitz, *J. Org. Chem.*, , DOI:10.1021/acs.joc.2c00549.
- 5 L. Gao, J. C. M. Meiring, Y. Kraus, M. Wranik, T. Weinert, S. D. Pritzl, R. Bingham, E. Ntoulou, K. I. Jansen, N. Olieric, J. Standfuss, L. C. Kapitein, T. Lohmüller, J. Ahlfeld, A. Akhmanova, M. O. Steinmetz and O. Thorn-Seshold, *Cell Chem. Biol.*, 2021, **28**, 228-241.e6.
- 6 N. Mardirossian and M. Head-Gordon, *Phys. Chem. Chem. Phys.*, 2014, **16**, 9904–9924.
- 7 F. Weigend and R. Ahlrichs, *Phys. Chem. Chem. Phys.*, 2005, **7**, 3297–3305.
- 8 F. Neese, *WIREs Comput. Mol. Sci.*, 2012, **2**, 73–78.
- 9 F. Neese, *Wiley Interdiscip. Rev. Comput. Mol. Sci.*, 2022, **12**, 1–15.
- 10 S. Grimme, *Chem. - A Eur. J.*, 2012, **18**, 9955–9964.
- 11 S. Grimme, A. Hansen, S. Ehlert and J. M. Mewes, *J. Chem. Phys.*, , DOI:10.1063/5.0040021.
- 12 A. Klamt, V. Jonas, T. Bürger and J. C. W. Lohrenz, *J. Phys. Chem. A*, 1998, **102**, 5074–5085.
- 13 A. Klamt, *J. Phys. Chem.*, 1995, **99**, 2224–2235.
- 14 X-Area LANA 2.7.9.0 (STOE&Cie, 2022.)
- 15 G. M. Sheldrick, *Acta Crystallogr. Sect. A Found. Adv.*, 2015, **71**, 3–8.
- 16 G. M. Sheldrick, *Acta Crystallogr. Sect. C Struct. Chem.*, 2015, **71**, 3–8.
- 17 H. D. Flack, *Acta Crystallogr. Sect. A Found. Crystallogr.*, 1983, **39**, 876–881.
- 18 R. W. W. Hoof, L. H. Straver and A. L. Spek, *J. Appl. Crystallogr.*, 2008, **41**, 96–103.